Fish and Shellfish Immunology 84 (2019) 609–626

Contents lists available at ScienceDirect

Fish and Shellfish Immunology

journal homepage: www.elsevier.com/locate/fsi

Full length article

Integrative transcriptome analysis and discovery of genes involving in immune response of hypoxia/thermal challenges in the small abalone *Haliotis diversicolor*

Xin Zhang[a], Jialong Shi[a], Yulong Sun[a], Yusuf Jibril Habib[a], Huiping Yang[b], Ziping Zhang[a,*], Yilei Wang[c,**]

[a] College of Animal Sciences, Fujian Agriculture and Forestry University, Fuzhou, Fujian Province, 350002, China
[b] School of Forest Resources and Conservation, Institute of Food and Agricultural Sciences, University of Florida, 7922 NW 71st Street, Gainesville, FL, 32653, USA
[c] Fisheries College, Jimei University, Xiamen, 361021, China

ARTICLE INFO

Keywords:
Abalone
Transcriptome
Immune response
Hypoxia/thermal stress
NF-κB
RNAi

ABSTRACT

In recent years, the abalone aquaculture industry has been threatened by the deteriorating environmental conditions, such as hypoxia and thermal stress in the hot summers. It is necessary to investigate the molecular mechanism in response to these environmental challenges, and subsequently understand the immune defense system. In this study, the transcriptome profiles by RNA-seq of hemocytes from the small abalone *Haliotis diversicolor* after exposure to hypoxia, thermal stress, and hypoxia plus thermal stress were established. A total of 103,703,074 clean reads were obtained and 99,774 unigenes were assembled. Of the 99,774 unigenes, 47,154 and 20,455 had homologous sequences in the Nr and Swiss-Prot protein databases, while 16,944 and 10,840 unigenes could be classified by COG or KEGG databases, respectively. RNAseq analysis revealed that the differentially expressed genes (DEGs) after challenges of hypoxia, thermal stress, or hypoxia plus thermal stress were 24,189, 29,165 and 23,665, among which more than 3000 genes involved in at least 230 pathways, including several classical immune-related pathways. The genes and pathways that were involved in immune response to hypoxia/thermal challenges were identified by transcriptome analysis and further validated by quantitative real-time PCR and RNAi technology. The findings in this study can provide information on *H. diversicolor* innate immunity to improve the abalone aquaculture industry, and the analysis of the potential immune-related genes in innate immunity signaling pathways and the obtained transcriptome data can provide an invaluable genetic resource for the study of the genome and functional genes.

1. Introduction

Abalones are herbivorous marine gastropods in the family Haliotidae and have historically been collected as high-value seafood and decoration products by the coastal communities for thousands of years. Nowadays, abalone industry has shifted from wild caught to farmed harvest, and over 95% of abalone production on market comes from aquaculture in the following countries, including China (including Taiwan Province), South Africa, Korea, Australia, Chile, USA, New Zealand, and Mexico (www.fao.org) [1]. Among these countries, China has been on the leading position with over 300 abalone farms (the largest farm has a capacity of over 1000 tonnes of abalones annually), and the abalone farming production has been continually increasing from 9810 tonnes in 2003 to 127,967 tonnes in 2015 [2,3].

The small abalone *Haliotis diversicolor* is a species naturally distributed along the southern coast in China and is one of the two major aquaculture species (another one is the Pacific abalone *H. discus hannai*). In recent years, aquaculture of small abalones in China has been facing severe diseases and deteriorating environmental conditions, especially the hypoxia and thermal stress in hot summers [4–6], and these problems have threatened the abalone industry for a long time [7]. The high temperature in summer months could diminish the amount of dissolved oxygen, and accordingly cause changes of metabolic and respiratory rates of farmed abalones [8], which may be related with the summer high mortality and diseases.

In our previous studies, several immune-related genes, such as

* Corresponding author.
** Corresponding author.
E-mail addresses: zhangziping@fafu.edu.cn (Z. Zhang), ylwang@jmu.edu.cn (Y. Wang).

https://doi.org/10.1016/j.fsi.2018.10.044
Received 25 May 2018; Received in revised form 18 October 2018; Accepted 20 October 2018
Available online 23 October 2018

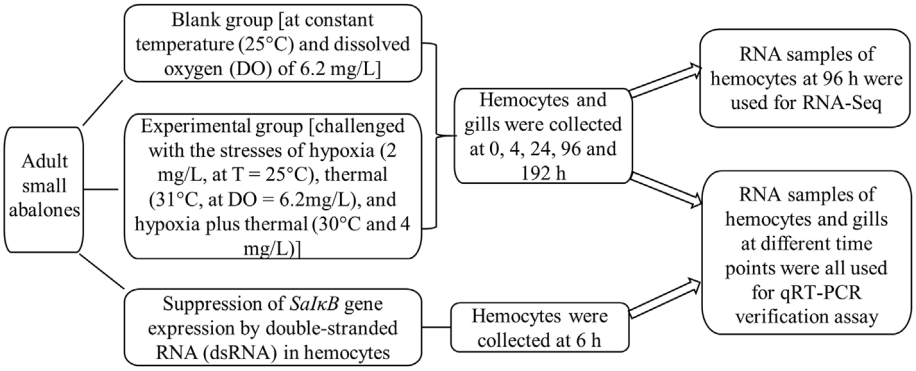

Fig. 1. The flow chart of experimental designation with sample treatment, tissue processing, data collection, and data analyses for transcriptome profiling and analyses in the small abalone *Haliotis diversicolor* in response to hypoxia, thermal stress, and hypoxia plus thermal stress.

Table 1
High-throughput RNA sequencing data for transcriptome assembly obtained from four libraries.[a]

Sample	All Reads Num	Unmapped Reads	Unique Mapped Reads	Multiple Mapped Reads	Mapping Ratio
BL-96h	23700078	2041080	20347859	1311139	91.39%
LO-96h	23942254	2496016	20120349	1325889	89.57%
HL-96h	17065366	1215674	15047901	801791	92.88%
HT-96h	34007970	2017007	30943295	1047668	94.07%

[a] These four libraries were constructed from RNA samples collected from the small abalone *Haliotis diversicolor* after 96-h exposure to hypoxia (low oxygen, LO-96h), thermal stress (high temperature, HT-96h), hypoxia plus thermal stress (HL-96h), and their control under normal conditions (BL-96h). The trinity software package (version 2.3.2) was used for this analysis.

macrophage migration inhibitory factor [9], macrophage expressed gene [10], insulin-like growth factor binding protein 7 [11], and interleukin-1 receptor-associated kinase 4 [12], have been cloned and characterized from *H. diversicolor*, and proved to be related with Rel/NF-κB signaling pathway [6], heat shock responses [5], HIF signaling pathway [4], PI3K-Akt signaling pathway [13], and toll-like receptor signaling pathway [14]. Under the stimulation of hypoxia and thermal stress, these genes could be up-regulated in *H. diversicolor* [4–6], indicating that the immune regulatory mechanisms of *H. diversicolor* could be modulated by thermal and hypoxia stresses. However, some mechanisms about the immune system in *H. diversicolor* are still unknown, such as the connections and cross-talks among different signaling pathways, and the regulations of the immune system by different stresses. It is well known that environmental stresses can cause primary responses at the level of gene expression [15], therefore, transcriptome profiles of abalones in responses to different stresses can provide insights for the mechanisms of immune regulations behind.

For vertebrate animals, the circulatory system connects different organs for nutrition material flow to maintain their functions (closed circulatory system). For molluscan shellfish, the circulatory system is

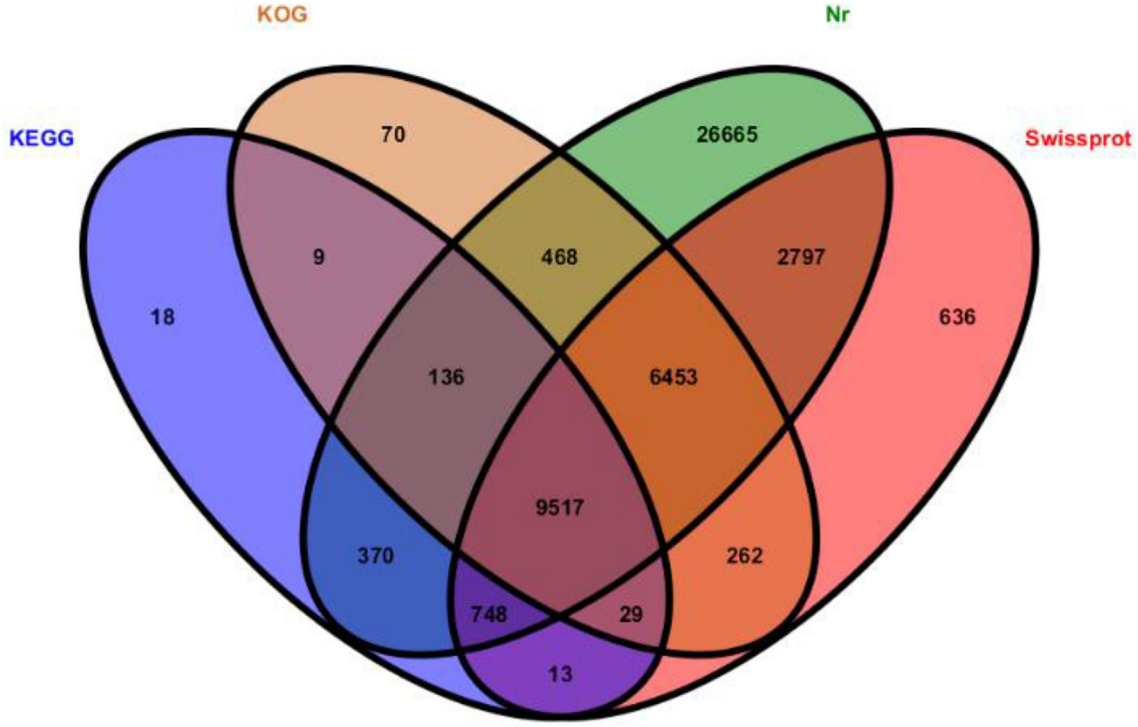

Fig. 2. Venn diagram of all 99,774 unigenes annotated against Nr, SwissProt, COG and KEGG databases in the small abalone *Haliotis diversicolor* in response to hypoxia, thermal stress, and hypoxia plus thermal stress. The number in each color block indicated the number of unigenes that was annotated by single or multiple databases.

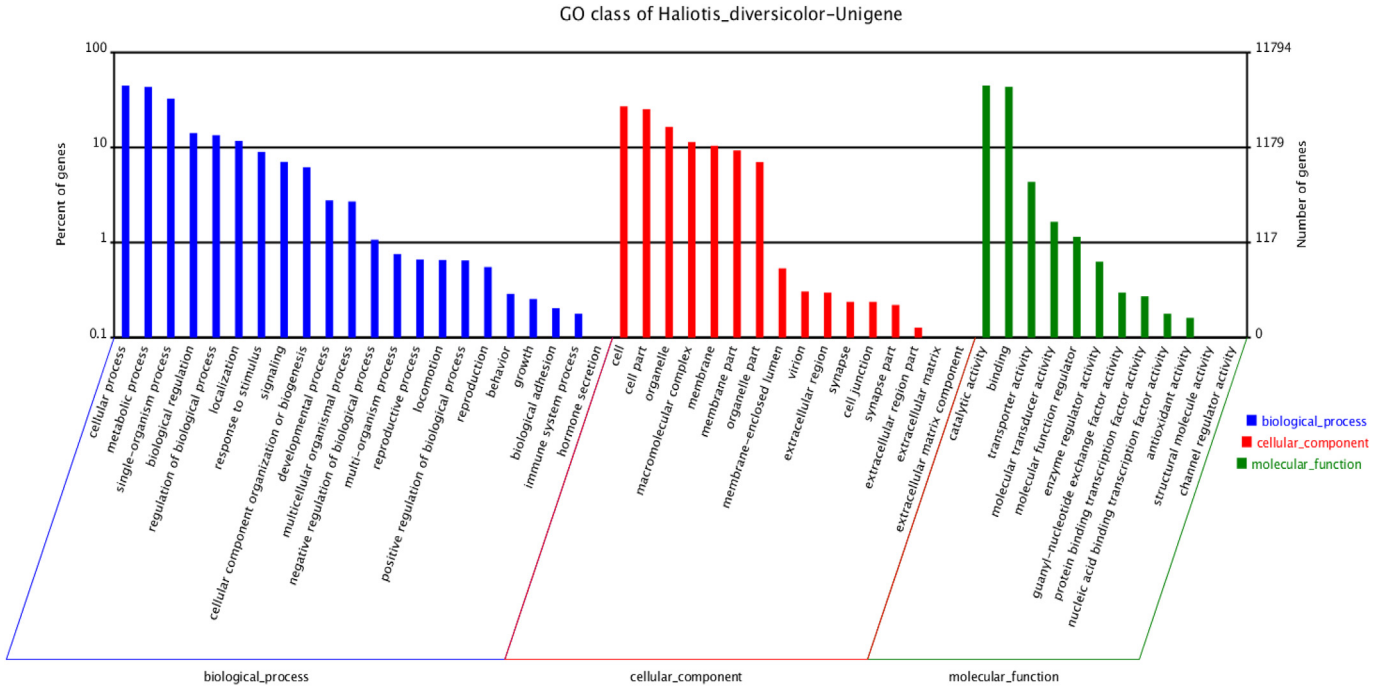

Fig. 3. GO function classification of the small abalone *Haliotis diversicolor* unigenes in response to hypoxia, thermal stress, or hypoxia plus thermal stress. A total of 11,794 unigenes can be classified into 50 categories.

open with simple heart, and blood (hemolymph) circulates through arteries, veins, and sinuses. Hemocytes in molluscan shellfish may function as blood cells in mammals for immune responses, and have three morphological types: agranular (hyaline cells), granular hemocytes, and small spherical cells (with big nuclei there may represent immature cells) [16]. Hemocytes were reported to play an important role in innate immune system in invertebrates [17,18], for example, hemocytes in the Pacific oyster *Crassostrea gigas* were found to participate in the internal defense through chemotaxis, recognition involving opsonin lectins, oxidative cytotoxic mechanisms, and homeostatic mechanisms [19–21]. To date, little information about their function at molecular level is available in abalones.

With fast development of DNA sequencing technology, genomic sequencing is becoming efficient and affordable. The first draft of genomic sequence for *H. discus hannai*, the aquaculture species in northern coastline in China, has been published [22]. Studies on transcriptome profiles have been performed in several abalone species, including *H. rufescens*, *H. laevigata*, *H. diversicolor*, and *H. midae* [23–29]. Gene expression during early embryo development in *H. diversicolor* was documented in details [26]; transcriptome profile of *H. midae* was assembled with more than 25 million short reads [23]; comparison of transcriptome profiles of wild and cultured populations was also performed in *H. midae* [29], and the potential functions of genes in response to environmental stresses and immunity were indicated in the greenlip abalone *H. laevigata* [25].

In this study, the goal was to develop the transcriptome profile of hemocytes from *H. diversicolor* in response to environmental stressors of hypoxia, thermal stress, and hypoxia plus thermal stress to understand the connections among the genes in immune system. The objectives were to: 1) develop transcriptome profile of hemocytes at 96 h exposure to hypoxia (2 mg/L, at T = 25 °C), thermal stress (31 °C, at DO = 6.2 mg/L), and hypoxia plus thermal stress (30 °C and 4 mg/L); 2) assemble a reference transcriptome and match against Uniprot, Gene ontology (GO), and Kyoto Encyclopedia of Gene and Genome (KEGG) to annotate the gene functions; 3) evaluate the effects of hypoxia, thermal stress, and hypoxia plus thermal stress on the gene expression in hemocytes, and 4) analyze the expression of potential immune-related genes of different signaling pathways. Overall, this study will provide an invaluable understanding of immune genes and their response to hypoxia, thermal stress, and combination of hypoxia and thermal stress. To further validate an important pathway involved in immune response to hypoxia/thermal challenges in the small abalone, the expression of a key gene of the pathway was inhibited by RNAi in hemocytes, and then the expression of this gene and other genes of the pathway was assessed by quantitative real-time PCR (qRT-PCR). It is expected that the results in this study will be useful for summer-related disease diagnosis and control for small abalone aquaculture.

2. Materials and methods

2.1. Animals and sample collection

Adult small abalones (body length 6.10 ± 0.50 cm, body weight 18.75 ± 2.50 g; n = 400) were purchased from Hongyun Abalone Farm (Zhangpu, Zhangzhou, Fujian Province) in July 2015. After arriving at the laboratory, these abalones were maintained in a recirculating system with a sand-filter at consistent temperature (25 °C) and dissolved oxygen (DO, 6.2 mg/L), and were fed with sea tangle (*Laminaria japonica*) once a day [6]. After 7 days of acclimation, the abalones were randomly separated into four groups with 100 individuals in each group for the following treatments of: 1) *Control*. T = 25 °C and dissolved oxygen (DO) = 6.2 mg/L; 2) *Hypoxia*. T = 25 °C and DO = 2 mg/L; 3) *Thermal stress*. T = 31 °C, DO = 6.2 mg/L, and 4) *Hypoxia plus thermal stress*. T = 30 °C and DO = 4 mg/L. These treatment conditions were determined based on our previous studies [4–6]. During treatments, dissolved oxygen and water temperature were controlled by using a whole set of temperature-controlled equipment (Cole-Parmer, Vernon Hills, IL USA). In addition, a handheld oxygen meter (YSI Environmental Model 556, Yellow Springs, OH, USA) was used to monitor the water temperature, pH, and dissolved oxygen throughout the treatment. After 0, 4, 24, 96, and 192 h of treatments, eight abalones from each group were randomly sampled for gill and hemolymph collection (see Fig. 1 the flow-chart of sampling). Gills were dissected and immediately frozen in a 2.0-ml

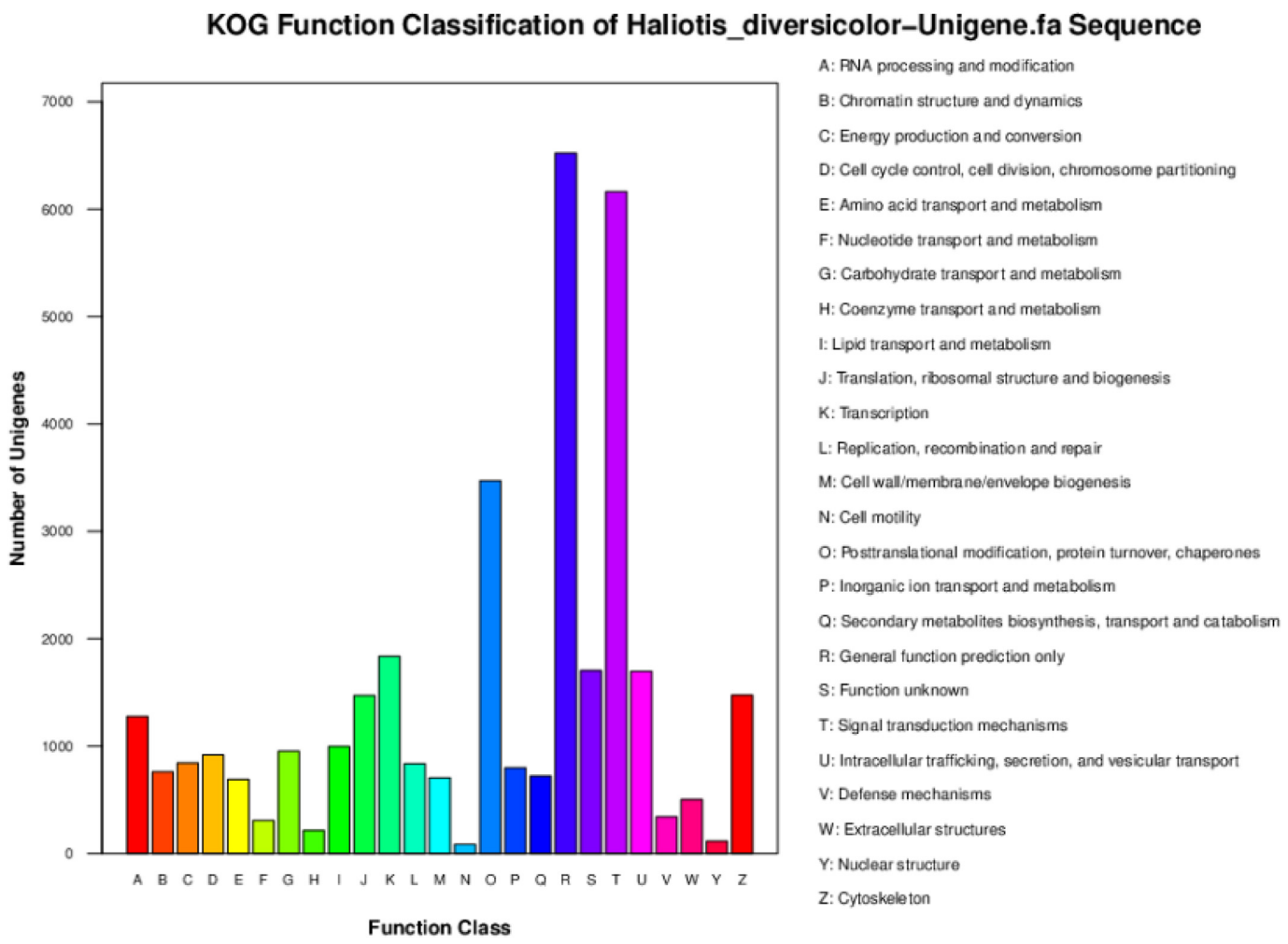

Fig. 4. The cluster of orthologous groups (COG) classification of the small abalone *Haliotis diversicolor* unigenes in response to hypoxia, thermal stress, or hypoxia plus thermal stress. A total of 35,379 unigenes were annotated into 25 categories.

cryovials in liquid nitrogen until use for analysis. Hemolymph was collected from each abalone with the foot cutting off and released in a 2.0-ml centrifugation tube. Hemocytes were isolated by centrifugation of hemolymph at 2000 g at 4 °C for 10 min and discarded of the supernatant, and frozen immediately in liquid nitrogen until use for RNA isolation.

2.2. Isolation of total RNA

Total RNAs were extracted from hemocytes and gills using Trizol reagent (Thermo Fisher Scientific, Grand Island, NY, USA) according to the manufacture's protocol. The quality of total RNAs was checked by agarose gel electrophoresis and spectrophotometry (Nano Drop ND-1000, Thermo Fisher Scientific, Wilmington, DE, USA).

2.3. Reverse transcription and illumina sequencing

The RNA samples of hemocytes and gills at different time points were used for qRT-PCR verification assay. Meanwhile, The RNA samples of hemocytes at 96 h were used for transcriptome profile analysis. The cDNA was synthesized in a system, including 2 μg total RNA, 2 μL 10 μM Random primers, and 1 μL M-MLV reverse transcriptase (Promega, Madison, WI, USA), and diluted by 10-fold and 100-fold, and stored at −20 °C until use after quality checking.

RNA-Seq was performed at the Gene Denovo Biotechnology Co. (Guangzhou, Guangdong, China). The mRNA was enriched by Oligo (dT) beads after the total RNA was extracted. The enriched mRNA was fragmented into short fragments using fragmentation buffer, and reversely transcribed into cDNA with random primers. Second-strand cDNA were synthesized by DNA polymerase I, RNase H, dNTP and buffer. The cDNA fragments were purified with QIAquick PCR extraction kit, end repaired, poly (A) added, and ligated to Illumina sequencing adapters. The ligation products were size selected by agarose gel electrophoresis, PCR amplified, and then, libraries were sequenced on an Illumina Hiseq 2500 platform (Illumina, USA) and paired-end reads were generated. Ultimately, four cDNA libraries derived from hemocytes obtained under normal (BL-96h), hypoxia (LO-96h), thermal stress (HT-96h) and hypoxia plus thermal stress (HL-96h) have been constructed by using Illumina paired-end sequencing technology.

2.4. De novo assembly and annotation

Trinity software (version 2.3.2) was used for *de novo* transcriptome assembly without reference genome. The sequence reads have been cleaned by removing adaptor sequences, ambiguous 'N' nucleotides (with the ratio of 'N' to be more than 10%), and low quality sequences (with quality score less than 5) [30].

For annotation, non-redundant sequences were subjected to public databases, including the non-redundant protein (Nr) and non-redundant nucleotide (Nt) databases at NCBI (http://www.ncbi.nlm.nih.gov/), Swiss-Prot (http://www.ebi.ac.uk/uniprot/), Gene Ontology (GO) (http://www.geneontology.org/), Clusters of Orthologous Groups

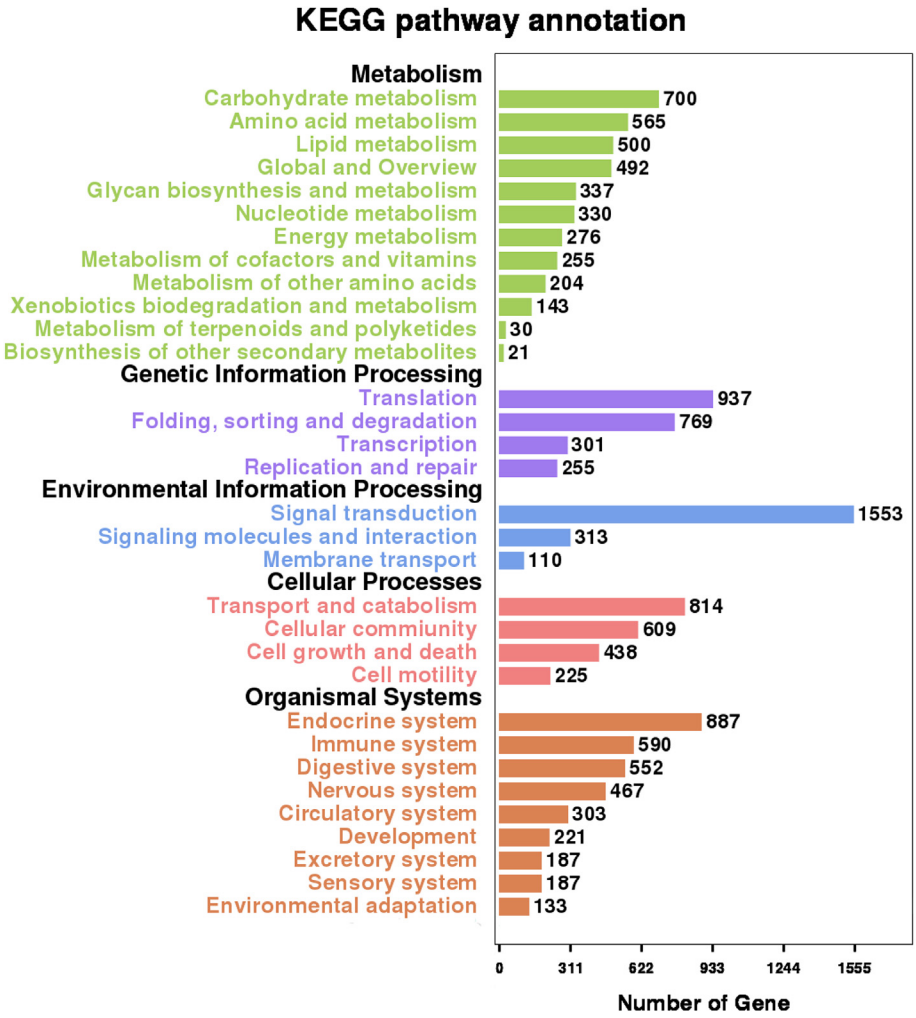

Fig. 5. The Kyoto Encyclopedia of Genes and Genomes (KEGG) classification of all assembled unigenes in the small abalone *Haliotis diversicolor*.

(COG) (http://www.ncbi.nlm.nih.gov/COG/), and Kyoto Encyclopedia of Genes and Genomes (KEGG) (http://www.genome.jp/kegg/). A priority order of alignments from Nr, Nt, KEGG, Swiss-Prot, GO and COG databases was followed when the results of different databases were conflicted.

2.5. Identification of differentially expressed genes

Differentially expressed genes (DEGs) were measured by counting tags from hypoxia/thermal treated samples against the control, which are normalized using the RNA Sequence Expected Maximization (RSEM) method [31]. Initially, reads from control sample were mapped to reference transcriptome and subjected to check the differential expression using trinity utility scripts (align_and_estimate_abundance.pl and abundance_estimates_to_matrix.pl) as instructed (http://trinityrnaseq.github.io/). From the edge R statistics files, regulated transcripts across libraries were filtered with default parameters (FDR < 0.05 and $|\log_2 FC| > 1$) using python scripts [32] to identify DEGs among different challenged samples.

2.6. Verification of immune-related genes by qRT-PCR

To verify the immunity responses to environmental stresses, twenty-one genes related to innate immunity in hemocytes were selected for verification by qRT-PCR with a 10 × SYBR Green Master Mix (Promega, Madison, WI, USA). Meanwhile, expression levels of these genes in gills, one of the main immune organs of invertebrate, were evaluated at different exposure times under each environmental stress. Gene-specific primers for DEGs (Supplementary file 1: Table S1) were used to amplify products of 200–300 bp from cDNA, and the housekeeping *β-actin* gene of *H. diversicolor* (Accession No. AY436644) was selected as controls [4,6,11]. qRT-PCR was carried out in a LightCycler480 Roche Realtime Thermal Cycler (Roche, Switzerland) according to the manual with a 20-μL reaction, containing 9 μL of 1:100 diluted original cDNA, 10 μL of 10 × SYBR Green Master Mix (Promega, Madison, WI, USA), and 0.5 μL of each primer (10 μM). The PCR cycling conditions were as follows: 95 °C for 1 min, 40 cycles at 95 °C for 15 s, and 60 °C for 1 min. Melting curves were also plotted (60 °C - 90 °C) to ensure that a single PCR product was amplified for each pair of primers. The comparative threshold cycle (CT method) (ΔCT = CT of target gene minus CT of *β-actin* gene and ΔΔCT = ΔCT of any sample minus calibrator sample) for the relative quantification of gene expression was used to calculate the relative expression levels of all these immune-related genes. Each sample was tested in triplicates for data collection. The statistical analysis of data at different stages was performed using the IBM SPSS Statistics 20 with T-test, and the significant level was set as $P < 0.05$.

2.7. Suppression of SaIκB gene expression by double-stranded RNA (dsRNA)

To elucidate the function of *SaIκB* in the intermolecular interaction of different genes, RNA interference was performed by using the dsRNA of *SaIκB*. The fragment of *SaIκB* was amplified by PCR using gene-

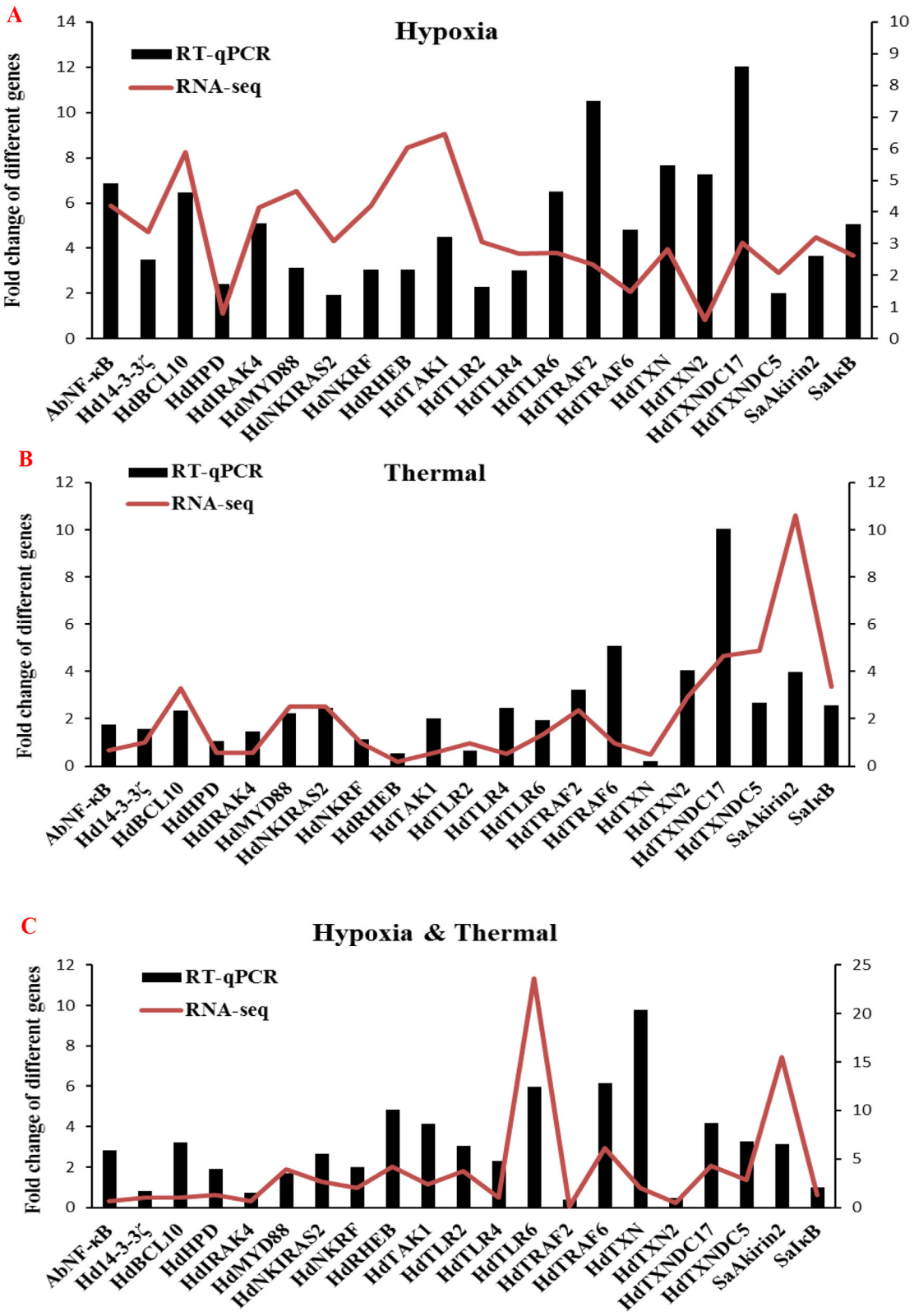

Fig. 6. Expression analysis of immune-relevant genes by RT-qPCR. **A** mRNA expression level of genes under hypoxia condition. **B** mRNA expression level of genes under thermal condition. **C** mRNA expression level of genes under hypoxia plus thermal condition. X-axis: Different genes, Y-axis: Fold change of each genes (fold change of RT-qPCR was on the left and fold change of RPKM was on the right). *β-actin* is as internal control gene.

specific primers (GenBank accession No. KF499084). Also, green fluorescent protein (GFP) gene from the pEGFP-N1 vector was amplified by PCR. The sequences of these primers were listed in supplementary file 1: Table S1 (note: the gray part of 5′ ends are T7 promoter sequences). Single-stranded RNA (ssRNA) was transcribed from the templates using T7 phage RNA polymerases (Promega, Madison, WI, USA) after the PCR products were purified and sequenced. DNase I (Promega, Madison, WI, USA) was used to degrade the DNA templates

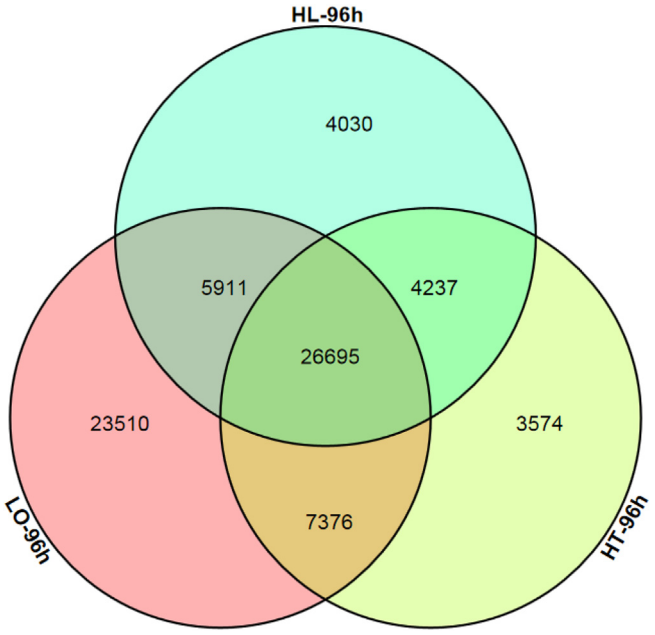

Fig. 7. Venn diagram of all unigenes under hypoxia, thermal stress, and hypoxia plus thermal treatment in the small abalone *Haliotis diversicolor*.

at a ratio of 1 U/μg. After being purified, the sense ssRNA and antisense ssRNA were mixed and annealed at 75 °C for 15 min, at 65 °C for 15 min, and then down to the room temperature at the rate of 0.1 °C/s.

The formation of dsRNA was tested by determining the size shift in agarose gel electrophoresis, and the concentration of dsRNA was measured by spectrophotometry. The dsRNA of *SaIκB* was used to silence experiment at a final concentration of 5 μg/mL directly to the hemocyte culture medium without any vehicle [33] with GFP dsRNA as control. The medium without any modifications was regarded as the blank control group. For each treatment, six replicates were produced. All samples were incubated at 27 °C for 6 h, and the hemocytes were harvested to detect the mRNA expression by qRT-PCR.

2.8. Visualization of gene expression data and construction of gene networks

A heatmap was created by using R Program (version 3.2.4, https://www.r-project.org/) to graphically visualize gene expression data, and the networks of immune-related genes were constructed using GeneMANIA app of Cytoscape 3.4.0.

3. Results

3.1. RNA sequencing and de novo assembly

A total of 103,704,122 raw reads (24,354,936 in BL-96h, 24,693,066 in LO-96h, 19,440,736 in HL-96h, and 35,215,384 in HT-96h) were obtained from the four libraries from the hemocytes, and clean reads were 100,858,126 (23,778,916 in BL-96h, 23,969,486 in LO-96h, 18,862,810 in HL-96h and 34,246,914 in HT-96h). After filtering the low-quality reads, short sequences, and low-complexity sequences, an average of Q30 (equal to 95.21%) was left for *de novo* transcriptome assembly. Assembly statistics of the transcriptome of the four samples were listed in Table 1. After removing the redundant data,

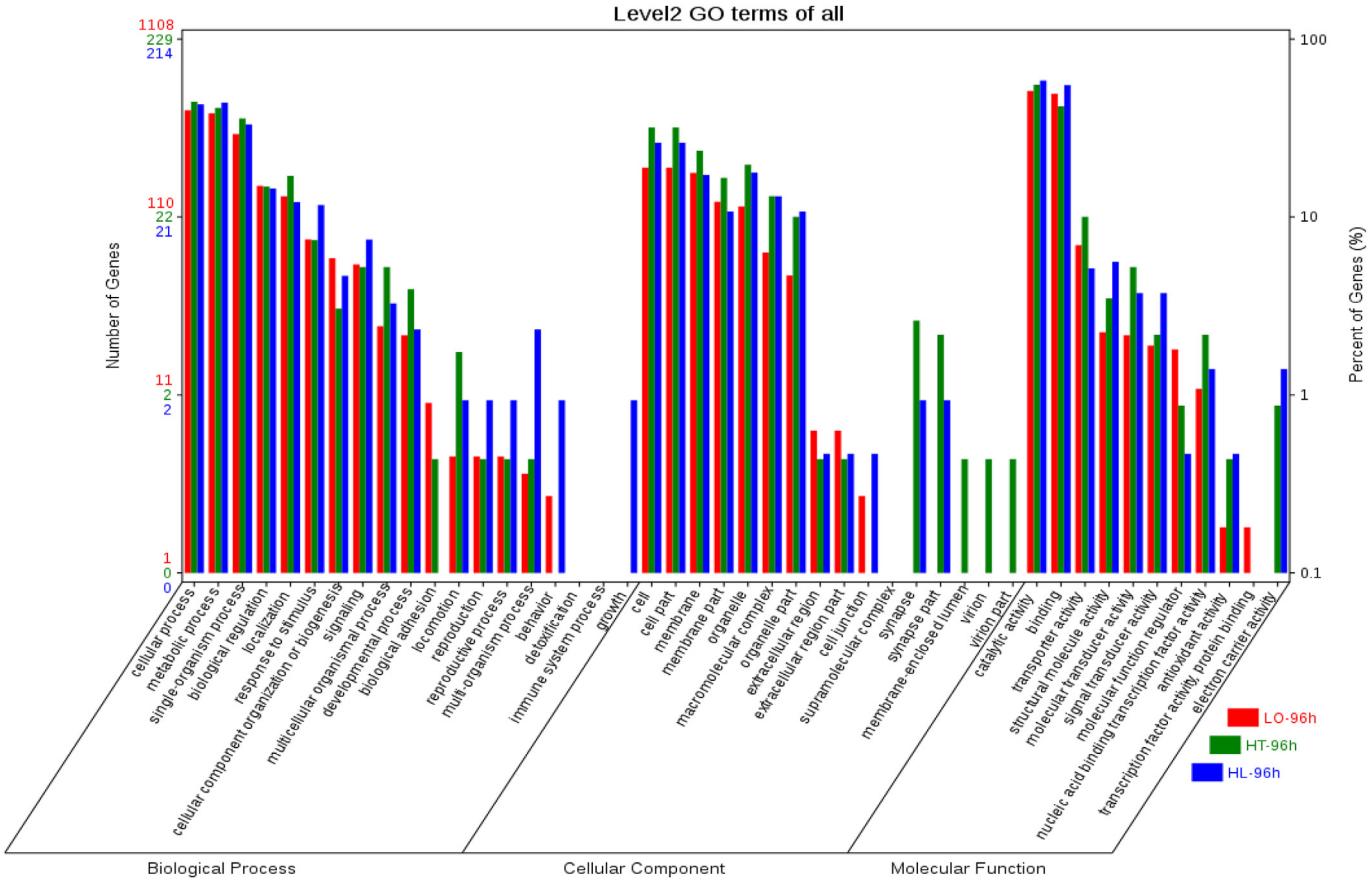

Fig. 8. GO function classification of the specific expressed genes under hypoxia, thermal stress, and hypoxia plus thermal treatment of the small abalone *Haliotis diversicolor*.

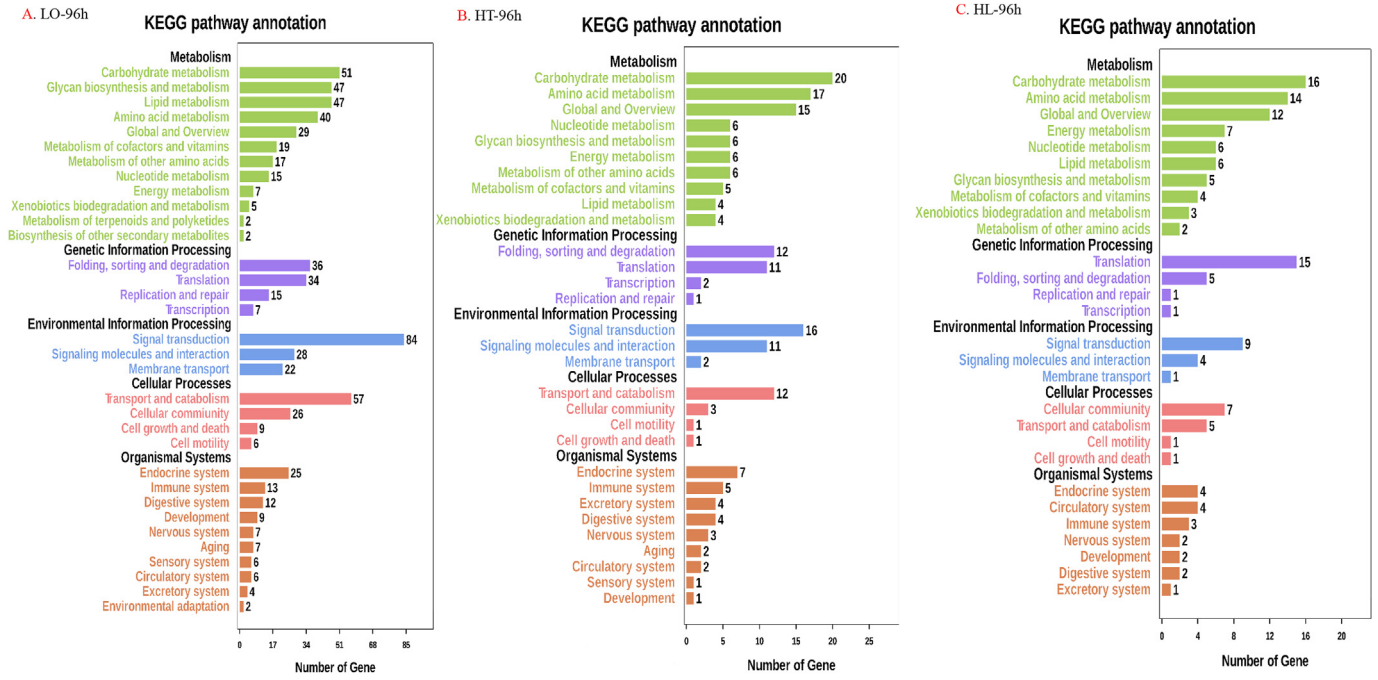

Fig. 9. The KEGG classification of the specific expressed genes under hypoxia, thermal stress, and hypoxia plus thermal treatment of the small abalone *Haliotis diversicolor*.

99,774 unigenes were assembled with an average length of 768.27 bp, a GC percentage of 41.08%, and an N50 value of 1414 bp (Table 1). All raw reads were submitted to the NCBI Short Read Archive database with the accession number SRP154122.

3.2. Gene function annotation

A total of 48,191 significant BLAST hits (48.3% of all unigenes) were obtained with 47,154 (97.85%) noted in NR, 16,944 (35.16%) in KOG, 10,840 (22.49%) in KEGG, and 20,455 (42.45%) in Swiss-Prot (Fig. 2). The GO functional analysis showed that 11,794 unigenes were successfully assigned into 50 categories of three major categories: biological process, cellular component, and molecular function (Fig. 3). Among the multitudinous categories of biological process, cellular process (5,210, 23.08%) was the most dominant group, followed by metabolic process (5,069, 22.46%) and single-organism process (3,815, 16.90%). For the cellular component category, cell (3,168, 24.80%) and cell part (2,965, 23.21%) was the dominant groups, followed by organelle (1,928, 15.10%) and macromolecular complex (1,337, 10.47%). For the category of molecular function, catalytic activity (5,218, 46.09%) was the most dominant group and 5082 (44.89%) of the unigenes were assigned to binding and transporter activity (509, 4.50%) (Fig. 3).

A total of 35,379 unigenes were annotated to 25 categories from the KOG annotation in which the cluster of General Functional Prediction only (R) represented the largest group (6,520, 18.43%), followed by Signal transduction mechanisms (T) (6,163, 17.42%) and post-translational modification, protein turnover, chaperon (O) (3,471, 9.81%). Meanwhile, 340 unigenes (0.96%) were assigned to defense mechanisms (V) (Fig. 4). In addition, the limited genome information on molluscan species and the insufficient sequences in the public databases lead to the poor annotation efficiency [34]. A total of 10,840 unigenes had significant matches in KEGG database and were assigned to five KEGG categories with 32 subclasses (Fig. 5).

3.3. Analysis of DEGs related to hypoxia, thermal stress, and hypoxia plus thermal stress and the validation of certain DEGs by qRT-PCR

The expression profiles of DGEs identified by RNA-seq analysis were verified by measuring the relative mRNA levels of twenty-one genes using qRT-PCR (supplementary file 1 Table S1). These results also showed a high consistency with the FPKM analysis of RNA-seq (Fig. 6-A, B, C).

The specific genes expressed under hypoxia, thermal stress, and hypoxia plus thermal stress in *H. diversicolor* were demonstrated in the Venn diagram (Fig. 7). Under hypoxia condition, a very high number of genes (23,510 genes) were identified as specifically expressed; under thermal stress, a total of 3574 genes expressed specifically, and under combination of hypoxia plus thermal stress, a total of 4030 genes were identified. The GO functional analysis showed that these specific expressed genes were successfully assigned into 46 categories of three major categories: biological process, cellular component, and molecular function (Fig. 8). In 'response to stimulus' process, the proportion of genes was almost the same between thermal and hypoxia condition, while this percentage was much higher under hypoxia plus thermal condition. And, these genes fell into the same pattern in the process of 'multi-organism process', 'reproduction' and 'reproductive process' (Fig. 8). In addition, the annotation of genes by KEGG database showed that different amounts of genes under hypoxia, thermal stress, and hypoxia plus thermal stress were enriched to the 'immune system' subclasses (Fig. 9-A, B, C).

In response to hypoxia, a total of 24,189 genes (after normalization) were significantly differentially expressed with 15,372 genes up-regulated and 8817 genes down-regulated (Fig. 10 A); In response to thermal stress, 29,165 genes were significantly differentially expressed with 6337 up-regulated and 22,828 down-regulated (Fig. 10 B), and in response to hypoxia plus thermal stress, 23,665 genes were differentially expressed with 7051 gene up-regulated and 16,614 gene down-regulated (Fig. 10C). Further comparison between HL-96h (hypoxia plus thermal stress) and LO-96h (hypoxia) indicated that 31,926 genes were expressed differentially, including 23,026 up-regulated and 8900 down-regulated (Fig. 10 D). Comparison between HT-96h (thermal

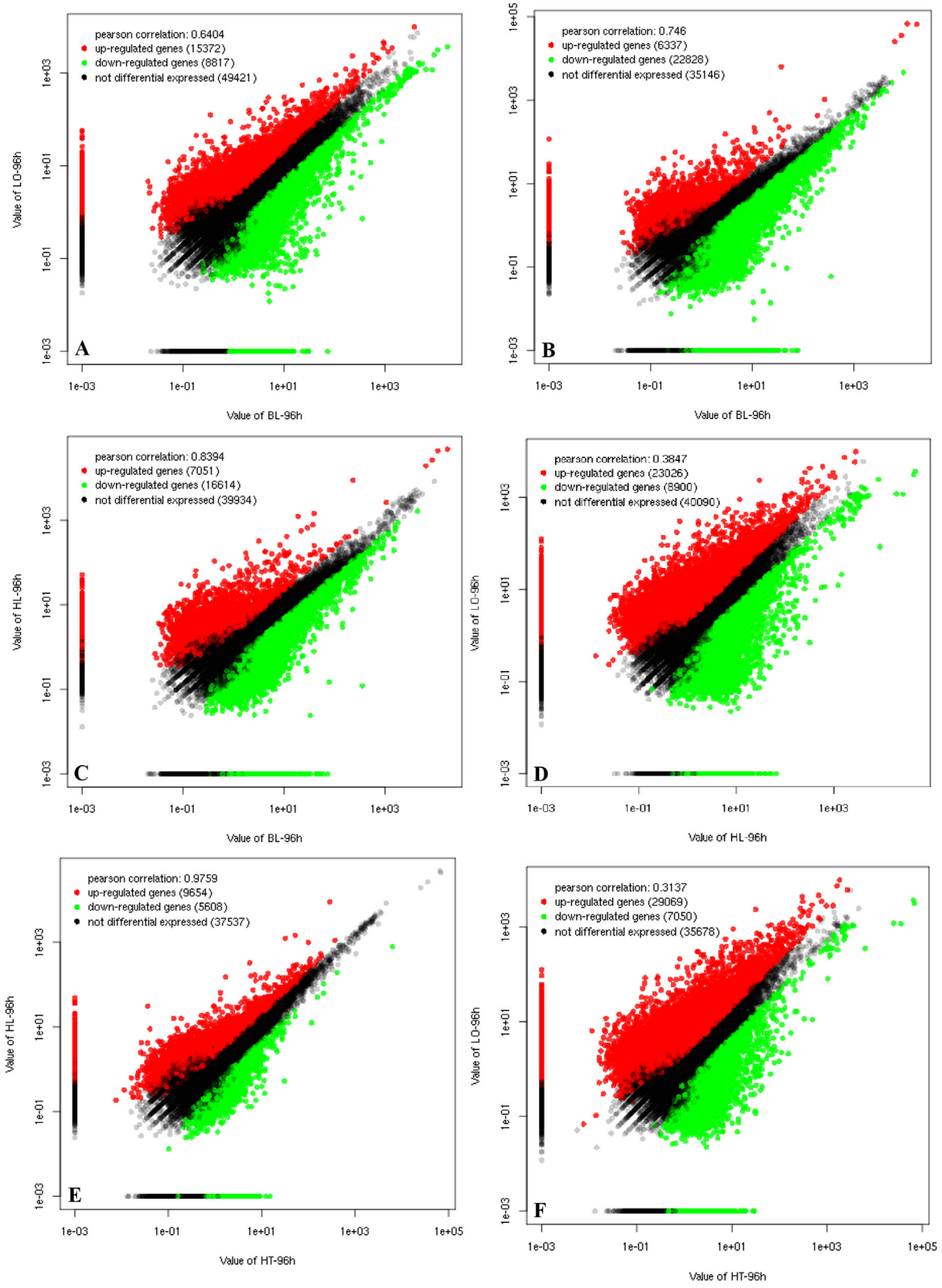

Fig. 10. Scatter diagram showed different expression levels of DEGs between pairwise comparisons under hypoxia, thermal stress, and hypoxia plus thermal treatment of the small abalone *Haliotis diversicolor*.

stress) and LO-96h (hypoxia) showed that 29,069 genes were up-regulated and 7050 were down-regulated (Fig. 10 E). Comparison between HT-96h (thermal stress) and HL-96h (hypoxia plus thermal stress) showed 9654 genes were up-regulated and 5608 genes were down-regulated (Fig. 10 F). The overall situation of all DEGs under hypoxia, thermal stress, and hypoxia plus thermal stress were shown in Fig. 11.

Function analyses using GO-TermFinder showed that all DEGs were categorized into more than twenty different biological processes, including 'immune system process' and 'response to stimulus' (Fig. 12).

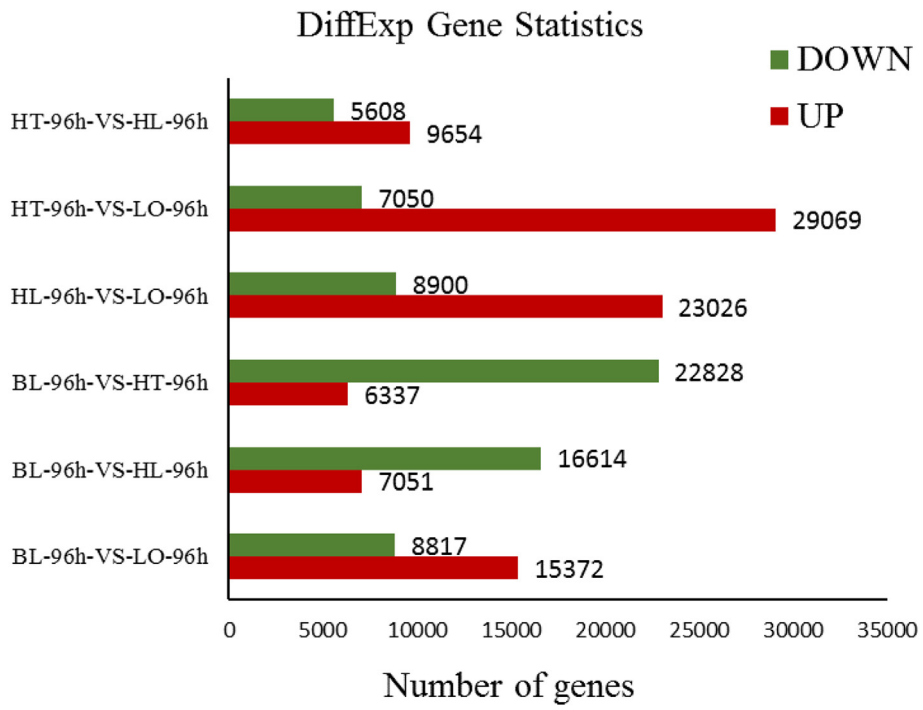

Fig. 11. The overall situation of the different expression levels of DEGs of all pairwise comparisons under hypoxia, thermal stress, and hypoxia plus thermal treatment in the small abalone *Haliotis diversicolor*.

All DGEs from the pairwise comparisons were mapped to KEGG for identification of the biological pathways in response to hypoxia, thermal stress, and hypoxia plus thermal stress, and a heatmap of these pathways was plotted by R (Fig. 13). It is indicated that immune-related pathways were enriched, such as Toll-like receptor signaling pathway, PI3K-Akt signaling pathway, and NF-κB signaling pathway.

With homogenization of all data, the heatmap exhibited different expression of immune-related genes in gills and hemocytes of *H. diversicolor*. Some of the same genes in the two tissues showed different expression pattern while the two tissues were divided into two separate clusters. It indicated that different regulatory modes of gene expression were activated in gills and hemocytes under different environmental stressors (Fig. 14-A, B, C).

3.4. Effect of dsRNA mRNA exposure assay for SaIκB gene expression

SaIκB, the key member of *NF-κB* signaling pathway, was inhibited by dsRNA in hemocytes. The qRT-PCR analysis of *SaIκB* indicated that exposure of hemocytes to dsRNA caused significant down-regulation of *SaIκB* mRNA at 6 h duration ($P < 0.05$, Fig. 15 A). With the interference of *SaIκB* gene, the mRNA expression analysis of other 20 genes indicated that 11 of them, including *AbNF-κB*, *SaAkirin2*, *Hd14-3-3ζ*, *HdRHEB*, *HdNKIRAS2*, *HdNKRF*, *HdTXN*, *HdTXN2*, *HdTXNDC5*, *HdTXNDC17* and *HdHPD,* changed significantly compared to internal control, the green fluorescent protein, and blank controls ($P < 0.05$, Fig. 15 A). However, no significant changes were detected in the mRNA expression of *HdBCL10*, *HdIRAK4*, *HdTAK1*, *HdMYD88*, *HdTRAF6*, *HdTRAF2*, *HdTLR2*, *HdTLR4* and *HdTLR6* ($P > 0.05$, Fig. 15 B).

3.5. The molecular network of NF-κB signaling pathway constructed by cytoscape

The molecular network of the related genes in NF-κB signaling pathway constructed using Cytoscape software indicated the gene interaction at 96 h exposure to hypoxia, thermal stress, and hypoxia plus thermal stress (Fig. 16). Under thermal stress, the expressions of *HdTAK1* (*MAP3K7*), *HdNKIRAS2*, *HdTXN*, *HdTXNDC5,* and *HdBCL10* were up-regulated or down-regulated, and all other genes were up-regulated (Fig. 16A and B). Under hypoxia shock, some genes were down-regulated in gills but up-regulated in hemocytes (Fig. 16C and D). Under hypoxia plus thermal stress, some genes showed complete opposite patterns of expression in gills and hymocytes (Fig. 16E and F).

Additionally, after *SaIκB* gene was inhibited, the molecular network of NF-κB signal pathway-related genes (Fig. 17) indicated that *SaIκB* had negative regulation effects on *AbNF-κB* and *SaAkirin2*, and inhibited the expression of *HdRHEB*, *HdNKIRAS2*, *HdNKRF*, *HdTXN*, *HdTXN2*, *HdTXNDC5*, *HdTXNDC17*, and *HdHPD* when it was inhibited by dsRNA. However, the expressions of *HdBCL10*, *HdIRAK4*, *HdTAK1*, *HdMYD88*, *HdTRAF6*, *HdTRAF2*, *HdTLR2*, *HdTLR4*, and *HdTLR6* were not affected by the interference of *SaIκB*.

4. Discussion

Immune regulations and response are of great value on resistance of diseases and environmental stresses for abalone aquaculture industry. Although the first draft genome in *H. discus hannai* has been published, studies were still constrained by the lack of sufficient knowledge in genomic resources of abalones [22]. RNA-Seq is an approach to understand the transcriptome profiling without requirement for genomic information by using deep sequencing technologies, and has become the main platform for transcriptome studies in non-model organisms [35,36].

In this study, 99,774 unigenes with an average length of 768 bp and an N50 of 1414 bp were obtained, and 48,191 unigenes (48.3%) were annotated successfully. After the analysis of BLASTX, the majority of unigenes matched closely with Pacific oysters *Crassostrea gigas* and California sea hares *Aplysia californica*, two molluscan species with the most expansive list of genes in the NCBI database [37–39]. Abundance of unannotated transcripts in this study may be related to the limited abalone genomic data. This study provides a valuable resource of genomic information and tools for abalones.

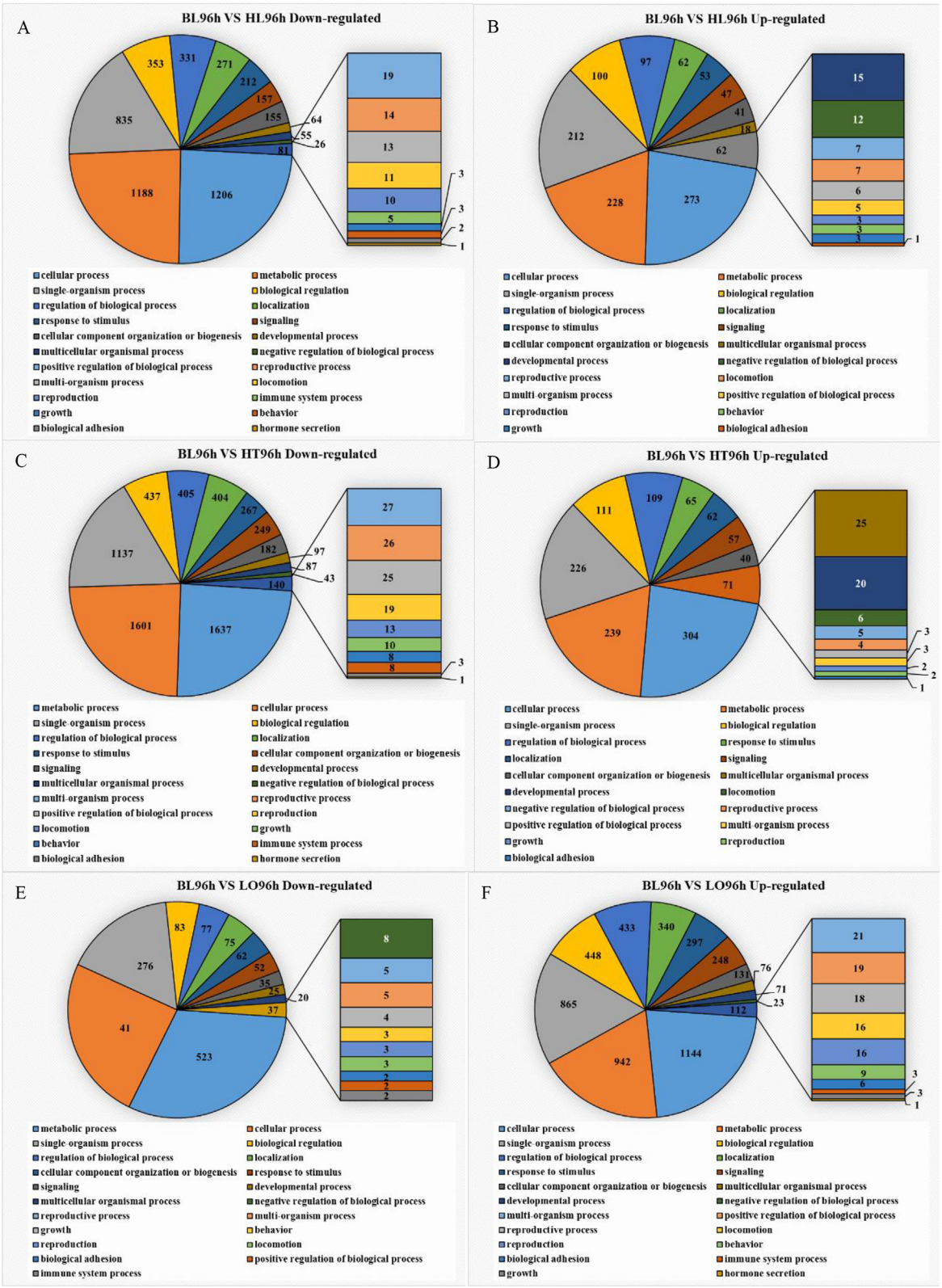

Fig. 12. Gene ontology (GO) enrichment analysis of the differently expressed genes in pairwise comparison: hypoxia (low oxygen, LO-96h, 2 mg/L at 25 °C), thermal stress (high temperature, HT-96h, 6.2 mg/L at 31 °C), hypoxia plus thermal stress (HL-96h, 4 mg/L at 30 °C), and their control under normal conditions (BL-96h, 6.2 mg/L at 25 °C) in the small abalone *Haliotis diversicolor*.

4.1. Different immune regulation caused by hypoxia, thermal stress, and hypoxia plus thermal stress

GO functional analysis showed that the number of specifically expressed genes in the hypoxia treatment group was more than that in the thermal stress and hypoxia plus thermal stress treatment group, but it was no contribute to the percentage of genes in category of 'response to stimulus'. Instead, a high percentage of genes in 'response to

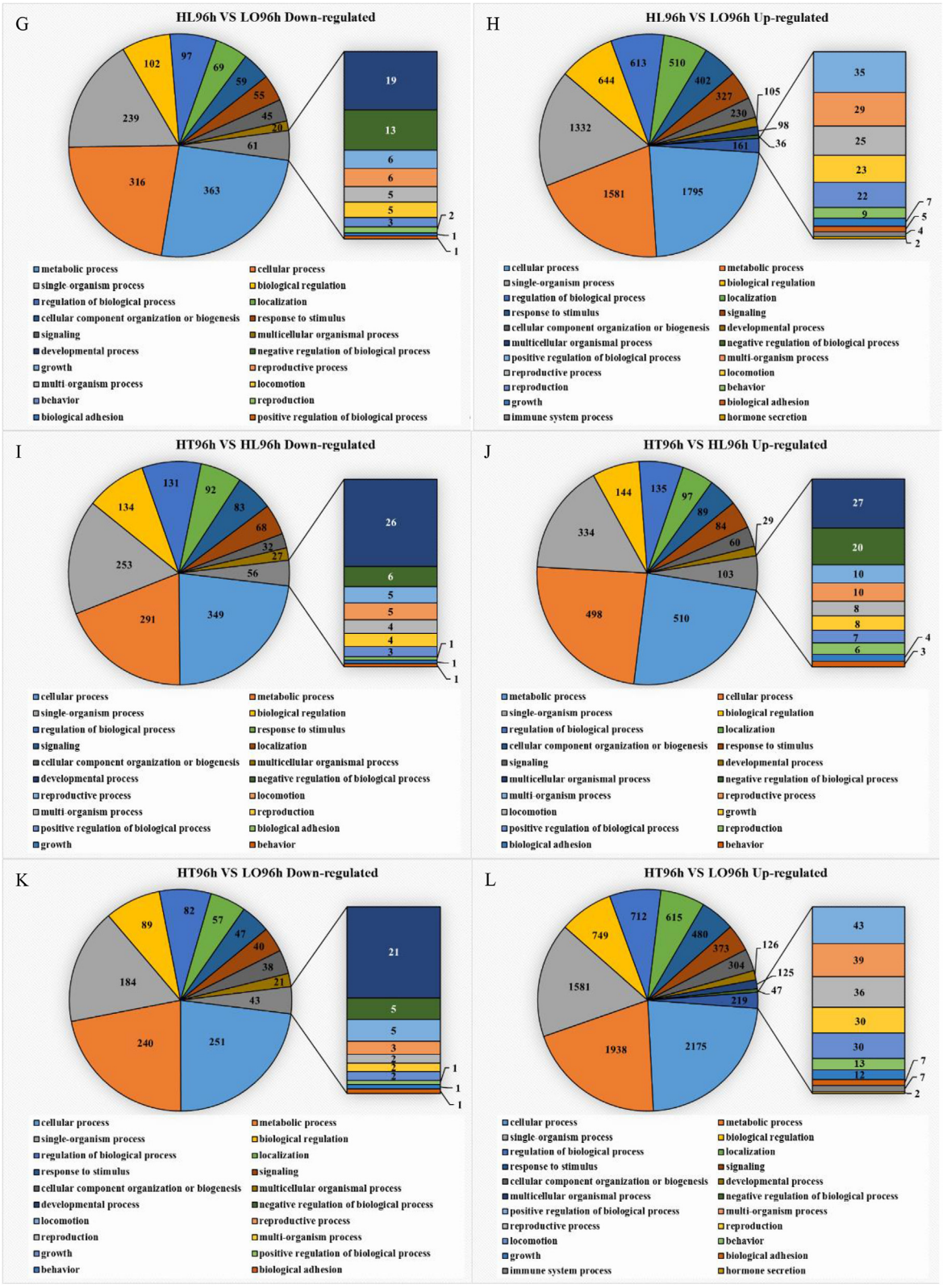

Fig. 12. (*continued*)

stimulus' process was from the genes responsive to hypoxia plus thermal stress. This phenomenon implied that combination of hypoxia and thermal stress could cause more immune regulation although hypoxia could only activate more genes to respond.

The annotation of DEGs by KEGG showed that several genes were enriched to the 'immune system' subclasses, which may take part in the immune defense of *H. diversicolor* under hypoxia, thermal stress, and hypoxia plus thermal stress. This result was similar to the findings in *C. gigas* [40], *Litopenaeus vannamei,* [41] and *Apostichopus japonicus* [42]. Although the number of DEGs enriched to 'immune system' subclass under hypoxia stress was more than that in the other two treated groups, the proportion of this number to all the DEGs in hypoxia group

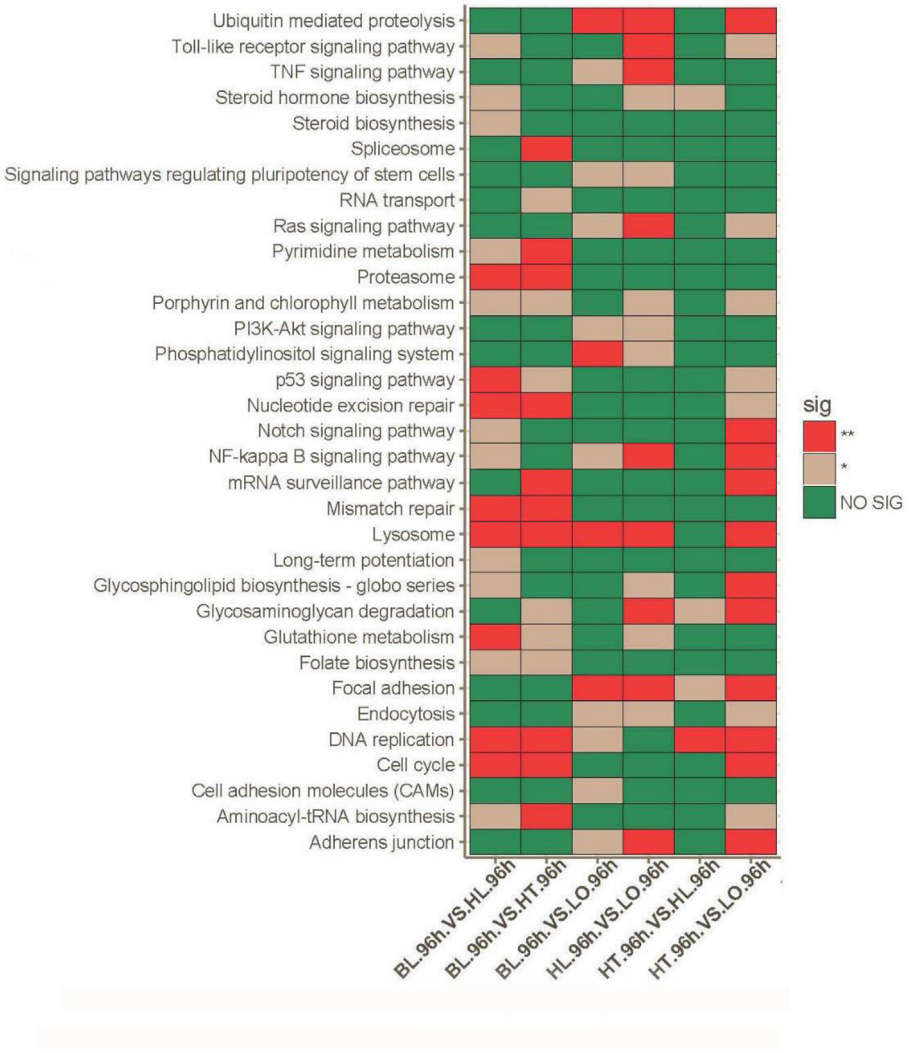

Fig. 13. The heatmap of all the pathways that were significantly enriched in different pairwise comparisons in the small abalone *Haliotis diversicolor*.

was almost same as hypoxia plus thermal stress group but was higher than in thermal stress group. This was the same as the result of GO functional analysis.

Furthermore, several innate immunity related pathways, such as NF-κB signaling pathway, Toll-like receptor signaling pathway, and PI3K-Akt signaling pathway, were enriched in the heatmap of KEGG. The pairwise comparisons of the unigenes under hypoxia, thermal stress, and hypoxia plus thermal stress revealed the different immune defense pathways. Six immune related pathways, including NF-κB, PI3K-Akt, Ras, TNF, Phosphatidylinositol, and Pluripotency of stem cells signaling pathways were significantly enriched under hypoxia stress. Under thermal stress, more metabolic pathways were significantly enriched while all these six immune-related pathways were not significant. Under hypoxia plus thermal stress, Toll-like receptor and NF-κB signaling pathway were significantly enriched. These results indicated that the immune defense mechanism activated by different environmental stressors, such as hypoxia, thermal stress, and hypoxia plus thermal stress in this study, could be through different regulatory pathways. It is worth mentioning that NF-κB signaling pathway played an important regulatory role both under hypoxia and hypoxia plus thermal stress. In our previous studies, Toll-like receptor signaling pathway [14] and PI3K-Akt signaling pathway [13] have also been confirmed being involved in the immune regulation of *H. diversicolor* under stimulations of hypoxia, thermal stress, hypoxia plus thermal stress.

4.2. Involvement of NF-κB signaling pathway in the immune regulation

NF-κB signaling pathway has been proved to be involved in innate immune response to bacterial infection and salinity stress in molluscan shellfish, including *Euprymna scolopes* [43], *Ruditapes philippinarum* [44], *M. meretrix* [45], *C. gigas* [46], *H. discus discus* [47], and *H. rufescens* [48]. Additionally, key members of this pathway have been identified being up-regulated significantly under thermal or hypoxia conditions in previous studies [6,49]. However, understanding of interaction among the genes within this pathway and the immunomodulation mechanism is still limited in molluscan shellfish.

In this study, the expression levels of more than twenty genes associated with NF-κB signaling pathway were quantified by qRT-PCR after treatment of hypoxia, thermal stress and hypoxia plus thermal stress. The heatmap established on these genes demonstrated their role on immune regulation to respond to the environmental stressors. For hypoxia stress, eleven genes (*AbNF-κB*, *HdBCL10*, *HdIRAK4*, *HdTLR6*, *HdTRAF2*, *HdTRAF6*, *HdTXN*, *HdTXN2*, *HdTXNDC17*, *SaIκB*, and *SaAkirin2*) were expressed at higher level, revealing that hypoxia exposure did stimulate the expression of key members of the NF-κB pathway. This agreed with the conclusion in previous studies about hypoxia [50,51]. For hypoxia or thermal stress, *HdTXNDC17* had the highest expression, however, at exposure to hypoxia plus thermal stress, *HdTXN* had the highest expression. This result indicated that the responses pathways in combined stresses were not simply additive effects.

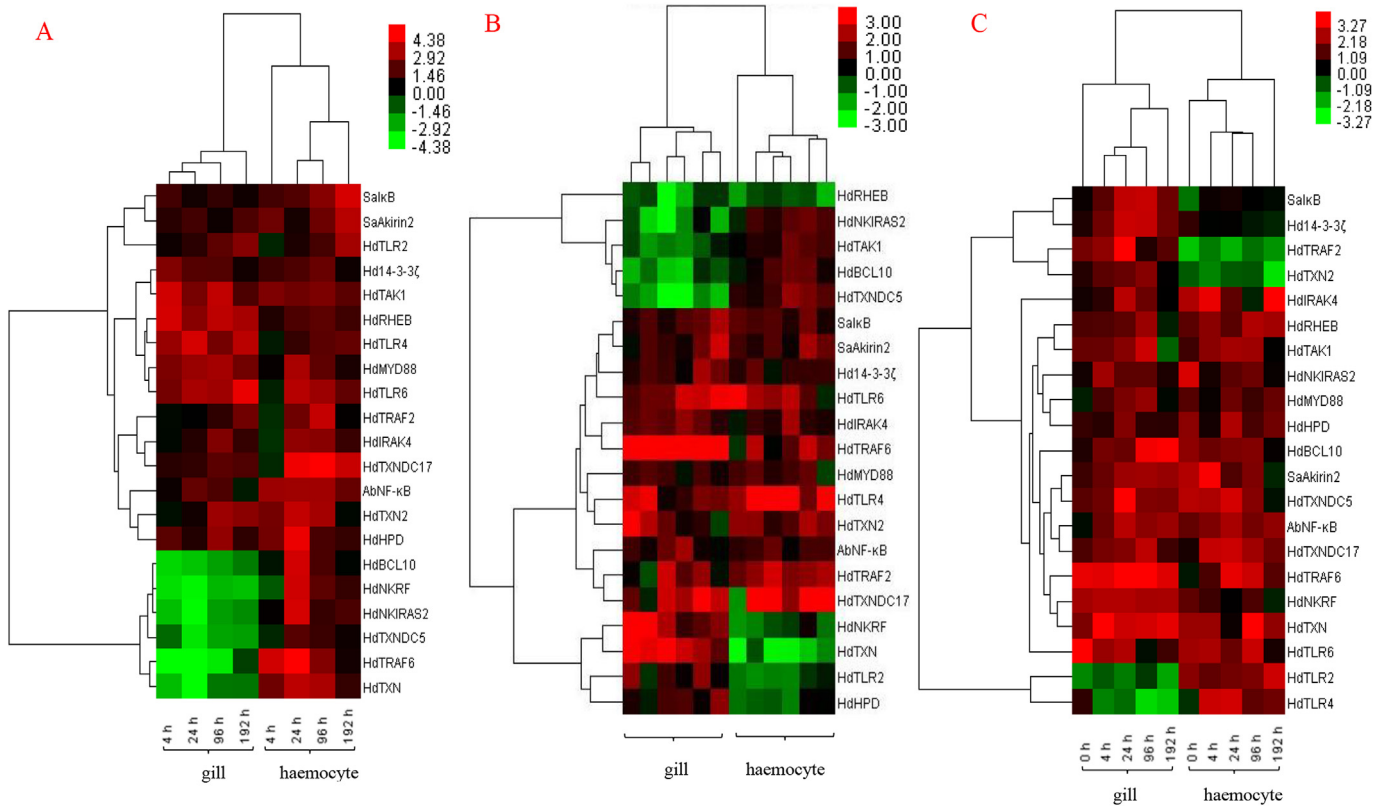

Fig. 14. The clustering analysis of immune-relevant genes under hypoxia, thermal stress, and hypoxia plus thermal treatment. **A** mRNA expression level of genes under hypoxia condition. **B** mRNA expression level of genes under thermal condition. **C** mRNA expression level of genes under hypoxia plus thermal condition. Time phase of thermal condition: 1 (temperature reach 28 °C), 2 (temperature reach 31 °C 0 h), 3 (3 h post thermal stress), 4 (24 h post thermal stress), 5 (96 h post thermal stress), 6 (192 h post thermal stress).

In fact, for hypoxia plus thermal stresses, five genes (*HdRHEB*, *HdTAK*1, *HdTLR6*, *HdTRAF6* and *HdTXN*) were expressed at highest levels, and three of them (*HdTLR6*, *HdTRAF6* and *HdTXN*) had a similar high expression under hypoxia stress. Controversially, five genes (*Hd14-3-3ζ*, *HdIRAK4*, *HdTXN2*, *HdTRAF2* and *SaIκB*) were expressed at the lowest level after hypoxia plus thermal exposure, demonstrating again that specific responses could be activated by different stresses.

Based on the analysis of the molecular network by Cytoscape and the gene expression patterns, the genes in gills and hemocytes in response to hypoxia, thermal stress, and hypoxia plus thermal stress could be generally classified into three categories:

1) The expressions of *HdTLR6*, *HdMYD88*, *HdTXNDC17* and *HdIRAK4* genes were significantly up-regulated in gills and hemocytes. The result implied that these four genes played key roles in direct transmission of signals through their up-regulated expression when exposed to hypoxia, thermal stress, and hypoxia plus thermal stress.
2) The expressions of *HdBCL10*, *HdTLR4*, *HdTRAF6*, *HdTXNDC5*, and *HdNKIRAS2* were significantly up-regulated in hemocytes, but significantly down-regulated in gills. Conversely, the expressions of *HdHPD*, *HdTRAF2,* and *HdTXN2* were significantly up-regulated in gills, but were significantly down-regulated in hemocytes. These results indicated that different tissues responded to stresses differently.
3) The expressions of *HdNKRF*, *HdTLR2,* and *HdTXN* were either up-regulated or down-regulated at different time points in gills and hemocytes.

Overall, the genes associated with NF-κB signaling pathway participated in the immunomodulation process to respond to hypoxia, thermal stresses and hypoxia plus thermal stress. Furthermore, immunomodulatory mechanisms could be different, independently or collaboratively, in hemocytes and gills to defend these environmental stressors.

4.3. RNA interference as a tool for study of gene function

RNA interference, including dsRNA, is one of the most widely used approach for studies of gene function and interaction, and has been applied in *Biomphalaria glabrata* for clarifying the function of genes in host-parasite interactions [52], also in *H. diversicolor* for the effect of IGFBP7 on cell proliferation [53]. RNAi is initiated by the enzyme Dicer, which cleaves long dsRNA molecules into short double-stranded fragments of 19–21 nucleotide siRNAs. Each siRNA is unwound into two ssRNAs, the passenger strand and the guide strand. The passenger strand is degraded and the guide strand is incorporated into the RNA-induced silencing complex (RISC). The well-studied outcome is post-transcriptional gene silencing. The activated RISC-siRNA complex scans, binds and degrades the complementary target mRNA present in the cell cytoplasm at a highly specific position relative to the 5′ end of the antisense strand, thus causing degradation of the complementary mRNA, which then leads to gene silencing [54]. As an important member of NF-κB signaling pathway, *SaIκB* gene was inhibited by dsRNA in hemocytes of *H. diversicolor* to understand the regulation of *SaIκB* on other genes in this pathway. It is well known that with the degradation of IκB the NF-κB complex can be freed to enter the nucleus and 'turned on' the expression of specific genes that have DNA-binding sites for NF-κB nearby. The genes activated by NF-κB indicated the physiological response, such as the inflammatory or immune response, a cell survival response, or cellular proliferation. Translocation of NF-κB to nucleus can be detected immunocytochemically and measured by laser scanning cytometry [55]. Additionally, NF-κB can turn on

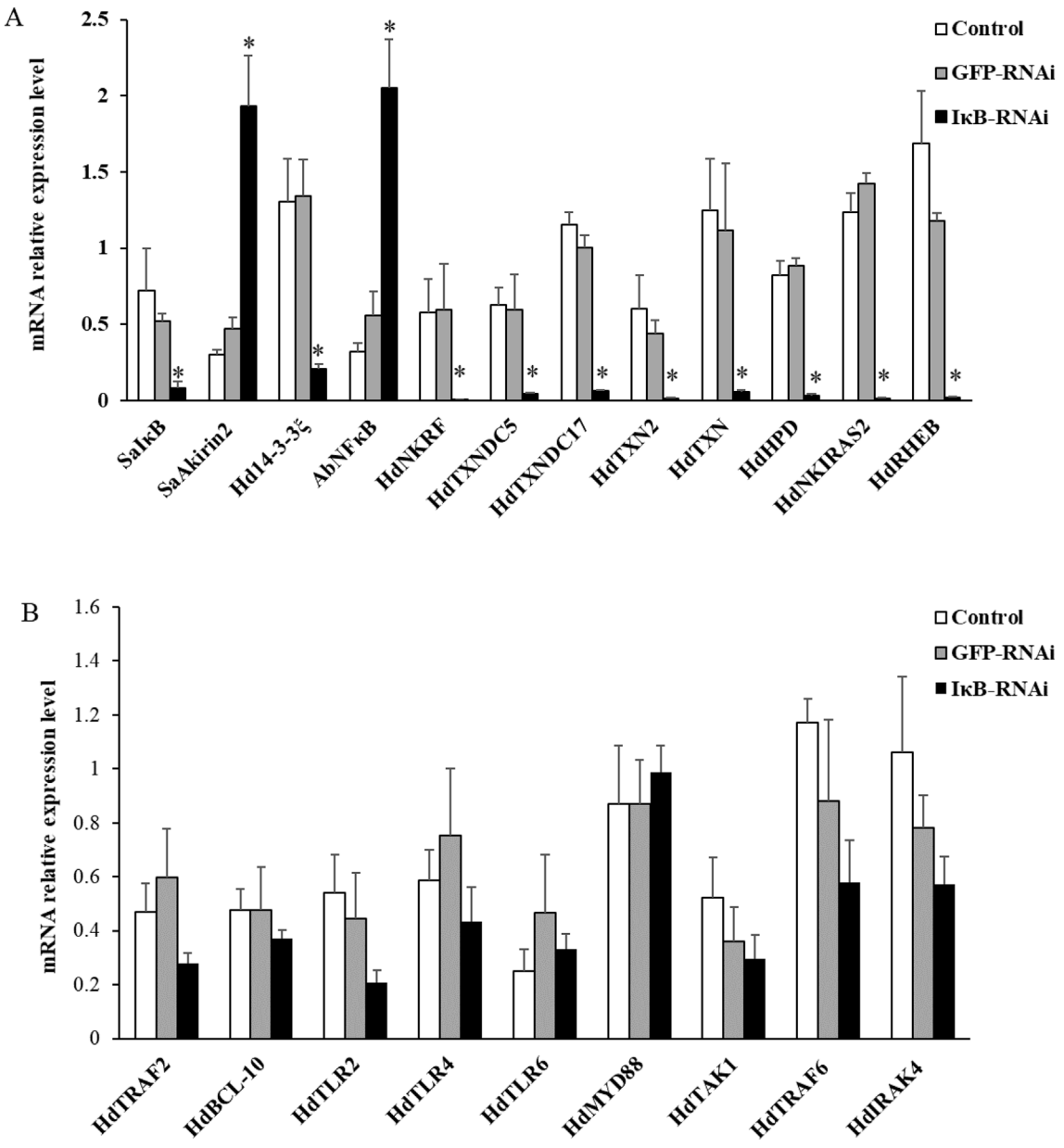

Fig. 15. The mRNA expression of immune-relevant genes in hemocytes after the interference of *SaIκB* with dsRNA incubation in the small abalone *Haliotis diversicolor*. **A** mRNA expression levels of 12 genes that changed significantly compared to internal control, the green fluorescent protein, and blank controls of genes after the interference of *SaIκB* ($P < 0.05$). **B** mRNA expression levels of 9 genes which had no significant difference compared to internal control, the green fluorescent protein, and blank controls of genes after the interference of *SaIκB* ($P > 0.05$). **X** axis represented different treatments. **Y** axis represented mRNA expression level of different genes. Significant difference between treated groups and control was indicated by a (*) at $p < 0.05$.

expression of its own repressor, IκBα, which can then re-inhibits NF-κB to form an auto feedback loop. This is also the oscillating levels of NF-κB activity [56]. In this study, qRT-PCR was used to detect the expression of *SaIκB* and other related genes in NF-κB signaling pathway. The full length of *SaIκB* cDNA has been cloned in the previous studies, which was 1748 bp with an open reading frame (ORF) of 1206 bp and encoding a protein of 401 amino acids. The analysis by the SMART program found that *SaIκB* contained six ankyrin repeats (158aa-187aa, 194aa-223aa, 227aa-259aa, 278aa-307aa, 312aa-342aa, 346aa-375aa) which were the typical features of the IκB in the C-terminal part and specific for binding of IκBs to the Rel-homology domain of NF-κB [6]. The dsRNA used to effect knockdown in this study was designed in the sequence-characterized region from 287bp to 673bp, which did not include regions that encode ankyrin repeats. The silence of *SaIκB* and upregulated expression of *AbNF-κB* and *SaAkirin2* indicated that *SaIκB* had a negative regulation effect on *AbNF-κB* and *SaAkirin2*. Meanwhile, the significant inhibition of *HdRHEB*, *HdNKIRAS2*, *HdNKRF*, *HdTXN*, *HdTXN2*, *HdTXNDC5*, *HdTXNDC17*, and *HdHPD* expression after silence of *SaIκB* indicated *SaIκB*'s critical role in the regulation of these genes. Furthermore, the unchanges of *HdBCL10*, *HdIRAK4*, *HdTAK1*, *HdMYD88*, *HdTRAF6, HdTRAF2*, *HdTLR2*, *HdTLR4*, and *HdTLR6* after silence of *SaIκB* showed that these genes could be located in the upstream of the NF-κB signaling pathway.

In addition, the analysis of RNA interference showed that *SaIκB* was also involved in the regulation of the thioredoxin family members *HdHPD,* a gene which is reported to participate in the regulation of NF-κB signal pathway [57–61]. Overall, the results of this study were complementary to the findings in the previous reports.

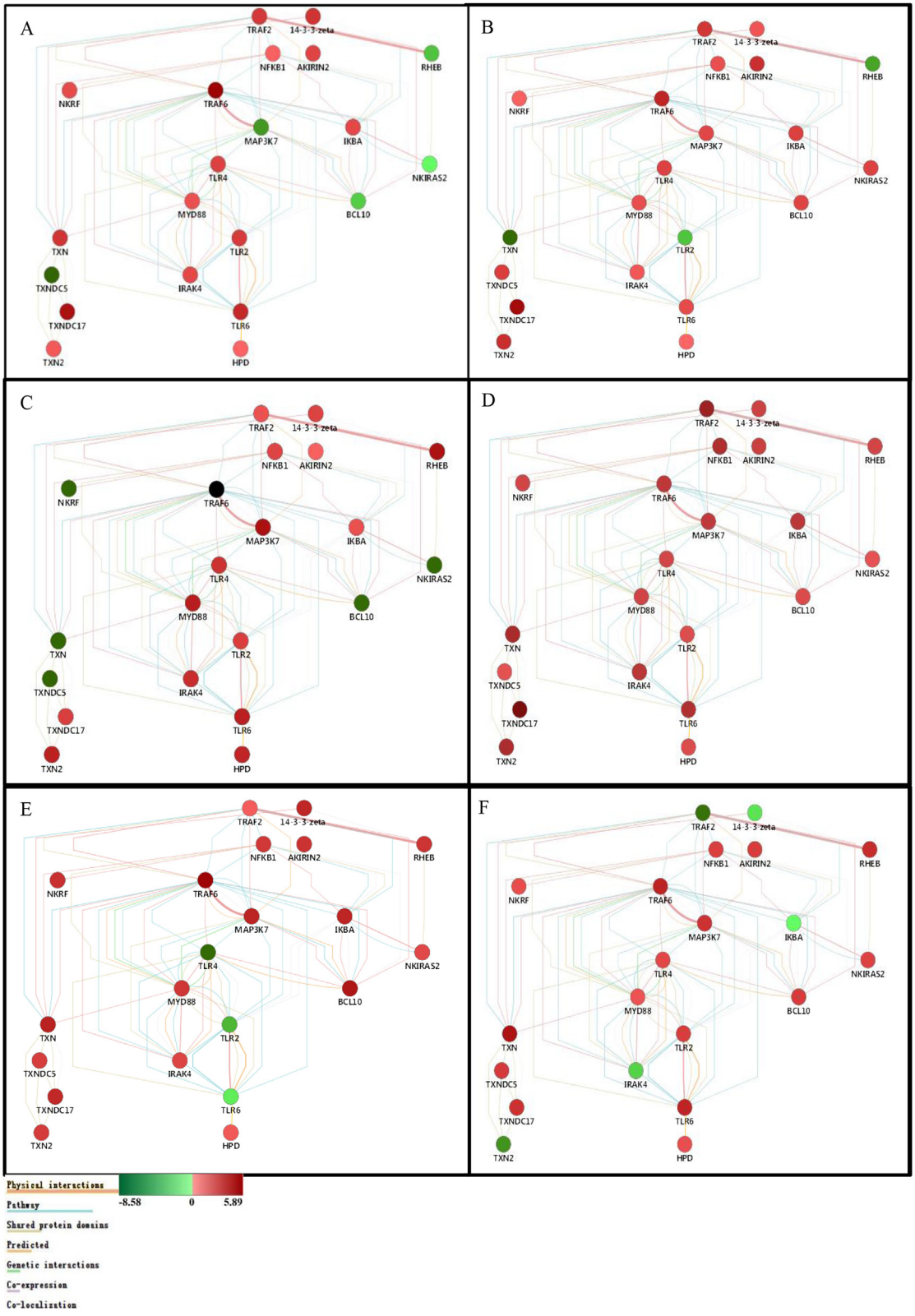

Fig. 16. The molecular network of the related genes in the *NF-κB signaling pathway* in response to thermal stress in gills (A) and hemocytes (B), hypoxia stress in gills (C) and hemocytes (D), and hypoxia plus thermal stress in gill (E) and hemocytes (F) of the small abalone *Haliotis diversicolor*.

5. Conclusions

Comparative transcriptome profiles of *H. diversicolor* in response to 96 h exposure to hypoxia, thermal stress, and hypoxia plus thermal stress were created. Important immune defense genes in the NF-κB signal pathway, including *SaIκB*, *AbNF-κB*, *SaAkirin2*, and *HdRHEB,* were identified. The interaction network of genes related to NF-κB signal pathway of *H. diversicolor* was constructed by using Cytoscape software for the first time. The silencing of *SaIκB* could upregulate the expression of *AbNF-κB* and *SaAkirin2* and downregulate the expression

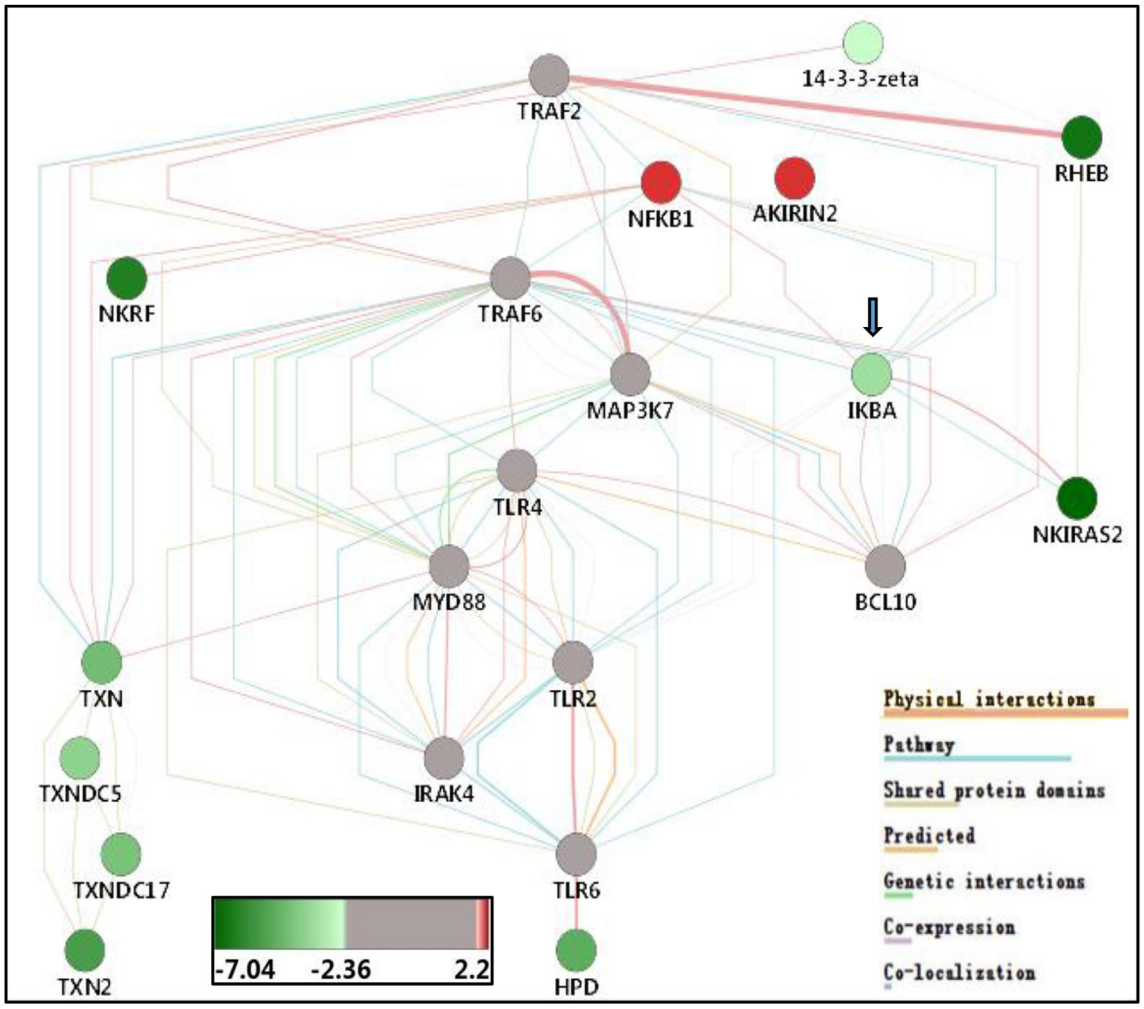

Fig. 17. The molecular network of the *NF-κB signaling pathway* related genes after *SaIκB* was inhibited in the small abalone *Haliotis diversicolor*. *SaIκB* was indicated by an arrow. Green represents the genes that were down-regulated significantly after *SaIκB* was inhibited. Red indicates the significantly up-regulated genes. Genes that were no significant difference after *SaIκB* was inhibited were indicated by gray. (For interpretation of the references to color in this figure legend, the reader is referred to the Web version of this article.)

of *HdRHEB*, *HdNKIRAS2*, *HdNKRF*, *HdTXN*, *HdTXN2*, *HdTXNDC5*, *HdTXNDC17*, and *HdHPD* in NF-κB signal pathway. This study will benefit the abalone aquaculture industry in overcoming the impediments of high mortality in hot summers.

Acknowledgments

This study was supported by the Natural Science Foundation of China (No. 41176152, No. 41006105), the Innovation Team Foundation of Jimei University (No. 2010A001), International Science and Technology Cooperation and Communication Grant of Fujian Agriculture and Forestry University (KXGH17019), and the Startup Fund of Fujian Agriculture and Forestry University (61201401201) for Dr. Ziping Zhang.

Appendix A. Supplementary data

Supplementary data to this article can be found online at https://doi.org/10.1016/j.fsi.2018.10.044.

References

[1] FAO, Fisheries and Aquaculture Statistics, (2017).
[2] P.A. Cook, The worldwide abalone industry, Mod. Econ. 5 (2014) 1181.
[3] P.A. Cook, Recent trends in worldwide abalone production, J. Shellfish Res. 35 (2016) 581–583.
[4] X.H. Cai, Y.T. Huang, X. Zhang, S.H. Wang, Z.H. Zou, G.D. Wang, et al., Cloning, characterization, hypoxia and heat shock response of hypoxia inducible factor-1 (*HIF-1*) from the small abalone *Haliotis diversicolor*, Gene 534 (2014) 256–264.
[5] Y.T. Huang, X.T. Cai, Z.H. Zou, S.H. Wang, G.D. Wang, Y.L. Wang, et al., Molecular cloning, characterization and expression analysis of three heat shock responsive genes from *Haliotis diversicolor*, Fish Shellfish Immunol. 36 (2014) 590–599.
[6] X. Zhang, Y.T. Huang, X.H. Cai, Z.H. Zou, G.D. Wang, S.H. Wang, et al., Identification and expression analysis of immune-related genes linked to Rel/NF-kappa B signaling pathway under stresses and bacterial challenge from the small abalone *Haliotis diversicolor*, Fish Shellfish Immunol. 41 (2014) 200–208.
[7] K.J. Wang, H.L. Ren, D.D. Xu, L. Cai, M. Yang, Identification of the up-regulated expression genes in hemocytes of variously colored abalone (*Haliotis diversicolor* Reeve, 1846) challenged with bacteria, Dev. Comp. Immunol. 32 (2008) 1326–1347.
[8] S.R. Vaquer, C.M. Duarte, Temperature effects on oxygen thresholds for hypoxia in marine benthic organisms, Global Change Biol. 17 (2011) 1788–1797.
[9] B.Z. Wang, Z.P. Zhang, Y.L. Wang, Z.H. Zou, G.D. Wang, S.H. Wang, et al., Molecular cloning and characterization of macrophage migration inhibitory factor from small abalone *Haliotis diversicolor* supertexta, Fish Shellfish Immunol. 27 (2009) 57–64.
[10] G.D. Wang, K.F. Zhang, Z.P. Zhang, Z.H. Zou, X.W. Jia, S.H. Wang, et al., Molecular cloning and responsive expression of macrophage expressed gene from small abalone *Haliotis diversicolor* supertexta, Fish Shellfish Immunol. 24 (2008) 346–359.
[11] N. Li, Z.P. Zhang, L.L. Zhang, S.H. Wang, Z.H. Zou, G.D. Wang, et al., Insulin-like growth factor binding protein 7, a member of insulin-like growth factor signal pathway, involved in immune response of small abalone *Haliotis diversicolor*, Fish Shellfish Immunol. 33 (2012) 229–242.
[12] H. Ge, G.D. Wang, L.L. Zhang, Z.P. Zhang, S.H. Wang, Z.H. Zou, et al., Molecular cloning and expression of interleukin-1 receptor-associated kinase 4, an important mediator of Toll-like receptor signal pathway, from small abalone *Haliotis*

diversicolor, Fish Shellfish Immunol. 30 (2011) 1138–1146.
[13] Y.L. Sun, X. Zhang, G.D. Wang, S. Lin, X.Y. Zeng, Y.L. Wang, et al., PI3K-AKT signaling pathway is involved in hypoxia/thermal-induced immunosuppression of small abalone *Haliotis diversicolor*, Fish Shellfish Immunol. 59 (2016) 492–508.
[14] H. Ge, G.D. Wang, L.L. Zhang, S.H. Wang, Z.H. Zou, S.F. Yan, et al., Characterization of interleukin-1 receptor-associated kinase 1 binding protein 1 gene in small abalone *Haliotis diversicolor*, Gene 506 (2012) 417–422.
[15] T.G. Evans, G.E. Hofmann, Defining the limits of physiological plasticity: how gene expression can assess and predict the consequences of ocean change, Phil. Trans. Biol. Sci. 367 (2012) 1733–1745.
[16] C.J. Secombes, T. Wang, S. Bird, Chapter 5 -Vertebrate cytokines and their evolution A2 - Malagoli, Davide. The Evolution of the Immune System, Academic Press, 2016, pp. 87–150.
[17] P.S. Gross, T.C. Bartlett, C.L. Browdy, R.W. Chapman, G.W. Warr, Immune gene discovery by expressed sequence tag analysis of hemocytes and hepatopancreas in the Pacific white shrimp, *Litopenaeus vannamei*, and the Atlantic white shrimp, *L. setiferus*, Dev. Comp. Immunol. 25 (2001) 565–577.
[18] Y. Gueguen, J.P. Cadoret, D. Flament, R.C. Barreau, A.L. Girardot, J. Garnier, et al., Immune gene discovery by expressed sequence tags generated from hemocytes of the bacteria-challenged oyster, *Crassostrea gigas*, Gene 303 (2003) 139–145.
[19] E. Bachere, D. Hervio, E. Mialhe, Luminol-dependent chemiluminescence by hemocytes of two marine bivalves, Ostrea edulis and *Crassostrea gigas*, Dis. Aquat. Org. 11 (1991) 173–180.
[20] A. Lacoste, M.C. De Cian, A. Cueff, S.A. Poulet, Noradrenaline and α-adrenergic signaling induce the *hsp70* gene promoter in mollusc immune cells, J. Cell Sci. 114 (2001) 3557–3564.
[21] A. Lacoste, A. Cueff, S.A. Poulet, P35-sensitive caspases, MAP kinases and Rho modulate β-adrenergic induction of apoptosis in mollusc immune cells, J. Cell Sci. 115 (2002) 761–768.
[22] B.H. Nam, W. Kwak, Y.O. Kim, D.G. Kim, H.J. Kong, W.J. Kim, et al., Genome sequence of pacific abalone (*Haliotis discus hannai*): the first draft genome in family Haliotidae, GigaScience 6 (2017) 1–8.
[23] P. Franchini, M. Van der Merwe, W.R. Roodt, Transcriptome characterization of the South African abalone *Haliotis midae* using sequencing-by-synthesis, BMC Res. Notes 4 (2011) 1.
[24] P. Wit, S.R. Palumbi, Transcriptome-wide polymorphisms of red abalone (*Haliotis rufescens*) reveal patterns of gene flow and local adaptation, Mol. Ecol. 22 (2013) 2884–2897.
[25] B.P. Shiel, N.E. Hall, I.R. Cooke, N.A. Robinson, J.M. Strugnell, De novo characterisation of the greenlip abalone transcriptome (*Haliotis laevigata*) with a focus on the heat shock protein 70 (*HSP70*) family, Mar. Biotechnol. 17 (2015) 23–32.
[26] Z.X. Huang, Z.S. Chen, C.H. Ke, J. Zhao, W.W. You, J. Zhang, et al., Pyrosequencing of *Haliotis diversicolor* transcriptomes: insights into early developmental molluscan gene expression, PloS One 7 (2012) e51279.
[27] A. Bester-Van Der Merwe, S. Blaauw, J. Du Plessis, R. Roodt-Wilding, Transcriptome-wide single nucleotide polymorphisms (SNPs) for abalone (*Haliotis midae*): validation and application using GoldenGate medium-throughput genotyping assays, Int. J. Mol. Sci. 14 (2013) 19341–19360.
[28] V. Valenzuela-Muñoz, M.A. Bueno-Ibarra, C.G. Escárate, Characterization of the transcriptomes of *Haliotis rufescens* reproductive tissues, Aquacult. Res. 45 (2014) 1026–1040.
[29] B. Picone, C. Rhode, R. Roodt-Wilding, Transcriptome profiles of wild and cultured South African abalone, *Haliotis midae*, Marine Genomics 20 (2015) 3–6.
[30] M.G. Grabherr, B.J. Haas, M. Yassour, J.Z. Levin, D.A. Thompson, I. Amit, et al., Full-length transcriptome assembly from RNA-Seq data without a reference genome, Nat. Biotechnol. 29 (2011) 644–652.
[31] B. Li, C.N. Dewey, RSEM: accurate transcript quantification from RNA-Seq data with or without a reference genome, BMC Bioinf. 12 (2011) 1.
[32] M.D. Robinson, D.J. McCarthy, G.K. Smyth, edgeR: a Bioconductor package for differential expression analysis of digital gene expression data, BMC Bioinf. 26 (2010) 139–140.
[33] Y. You, P. Huan, B. Liu, RNAi assay in primary cells: a new method for gene function analysis in marine bivalve, Mol. Biol. Rep. 39 (2012) 8209–8216.
[34] B. Dong, J.H. Xiang, Discovery of genes involved in defense/immunity functions in a haemocytes cDNA library from *Fenneropenaeus chinensis* by ESTs annotation, Aquaculture 272 (2007) 208–215.
[35] D.A. Hahn, G.J. Ragland, D.D. Shoemaker, D.L. Denlinger, Gene discovery using massively parallel pyrosequencing to develop ESTs for the flesh fly *Sarcophaga crassipalpis*, BMC Genomics 10 (2009) 234.
[36] D. Ma, H. Yang, L. Sun, M. Chen, Transcription profiling using RNA-Seq demonstrates expression differences in the body walls of juvenile albino and normal sea cucumbers *Apostichopus japonicus*, Chin. J. Oceanol. Limnol. 32 (2014) 34.
[37] B. Knudsen, A.B. Kohn, B. Nahir, C.S. McFadden, L.L. Moroz, Complete DNA sequence of the mitochondrial genome of the sea-slug, *Aplysia californica*: conservation of the gene order in Euthyneura, Mol. Phylogenet. Evol. 38 (2006) 459–469.
[38] L.L. Moroz, J.R. Edwards, S.V. Puthanveettil, A.B. Kohn, T. Ha, A. Heyland, et al., Neuronal transcriptome of Aplysia: neuronal compartments and circuitry, Cell 127 (2006) 1453–1467.
[39] G. Zhang, X. Fang, X. Guo, L. Li, R. Luo, F. Xu, et al., The oyster genome reveals stress adaptation and complexity of shell formation, Nature 490 (2012) 49–54.
[40] Q. Zhu, L. Zhang, L. Li, H. Que, G. Zhang, Expression characterization of stress genes under high and low temperature stresses in the Pacific oyster, *Crassostrea gigas*, Mar. Biotechnol. 18 (2016) 176–188.
[41] Y.H. Chen, F.H. Yuan, H.T. Bi, Z.Z. Zhang, H.T. Yue, K. Yuan, et al., Transcriptome analysis of the unfolded protein response in hemocytes of *Litopenaeus vannamei*, Fish Shellfish Immunol. 54 (2016) 153–163.
[42] Q. Gao, M. Liao, Y. Wang, B. Li, Z. Zhang, X. Rong, et al., Transcriptome analysis and discovery of genes involved in immune pathways from coelomocytes of sea cucumber (*Apostichopus japonicus*) after *Vibrio splendidus* challenge, Int. J. Mol. Sci. 16 (2015) 16347.
[43] M.S. Goodson, M. Kojadinovic, J.V. Troll, T.E. Scheetz, T.L. Casavant, M.B. Soares, et al., Identifying components of the NF-κB pathway in the beneficial *Euprymna scolopes-Vibrio fischeri* light organ symbiosis, Appl. Environ. Microbiol. 71 (2005) 6934–6946.
[44] Y. Lee, W.D. Wickamarachchi, I. Whang, M. Oh, N. Umasuthan, M. De Zoysa, et al., Immune response-related gene expression profile of a novel molluscan IkappaB protein member from Manila clam (*Ruditapes philippinarum*), Mol. Biol. Rep. 40 (2013) 1519–1527.
[45] Q. Yang, Z. Yang, H. Li, Molecular characterization and expression analysis of an inhibitor of NF-kappaB (IkappaB) from Asiatic hard clam *Meretrix meretrix*, Fish Shellfish Immunol. 31 (2011) 485–490.
[46] C. Montagnani, Y. Labreuche, J. Escoubas, Cg-IκB, a new member of the IκB protein family characterized in the pacific oyster *Crassostrea gigas*, Dev. Comp. Immunol. 32 (2008) 182–190.
[47] S.R. Kasthuri, I. Whang, U. Navaneethaiyer, B.S. Lim, C.Y. Choi, J. Lee, Molecular characterization and expression analysis of IkappaB from *Haliotis discus discus*, Fish Shellfish Immunol. 34 (2013) 1596–1604.
[48] V. Valenzuela-Muñoz, C. Gallardo-Escárate, Molecular cloning and expression of *IRAK-4, IL-17* and *IκB* genes in *Haliotis rufescens* challenged with *Vibrio anguillarum*, Fish Shellfish Immunol. 36 (2014) 503–509.
[49] L.H. He, X. Zhang, Y. Huang, H.P. Yang, Y.L. Wang, Z.P. Zhang, The characterization of RHEB gene and its responses to hypoxia and thermal stresses in the small abalone *Haliotis diversicolor*, Comp. Biochem. Physiol. B Biochem. Mol. Biol. 210 (2017) 48–54.
[50] C.T. Taylor, E.P. Cummins, The role of NF-κB in hypoxia-induced gene expression, Ann. N. Y. Acad. Sci. 1177 (2009) 178–184.
[51] C.T. Taylor, Interdependent roles for hypoxia inducible factor and nuclear factor-κB in hypoxic inflammation, J. Physiol. 586 (2008) 4055–4059.
[52] Y. Jiang, E.S. Loker, S.M. Zhang, In vivo and in vitro knockdown of *FREP2* gene expression in the snail *Biomphalaria glabrata* using RNA interference, Dev. Comp. Immunol. 30 (2006) 855–866.
[53] G. Wang, N. Li, L. Zhang, L. Zhang, Z. Zhang, Y. Wang, IGFBP7 promotes hemocyte proliferation in small abalone *Haliotis diversicolor*, proved by dsRNA and cap mRNA exposure, Gene 571 (2015) 65–70.
[54] D.S. Schwarz, G. Hutvágner, T. Du, Z. Xu, N. Aronin, P.D. Zamore, Asymmetry in the assembly of the RNAi enzyme complex, Cell 115 (2003) 199–208.
[55] A. Deptala, E. Bedner, W. Gorczyca, Z. Darzynkiewicz, Activation of nuclear factor kappa B (NF-κB) assayed by laser scanning cytometry (LSC), Cytometry 33 (1998) 376–382.
[56] D.E. Nelson, A.E.C. Ihekwaba, M. Elliott, J.R. Johnson, C.A. Gibney, B.E. Foreman, et al., Oscillations in NF-κB signaling control the dynamics of gene expression, Science 306 (2004) 704.
[57] K. Hirota, M. Murata, Y. Sachi, H. Nakamura, J. Takeuchi, K. Mori, et al., Distinct roles of thioredoxin in the cytoplasm and in the nucleus a two-step mechanism of redox regulation of transcription factor NF-κB, J. Biol. Chem. 274 (1999) 27891–27897.
[58] K. Hirota, M. Matsui, M. Murata, Y. Takashima, F.S. Cheng, T. Itoh, et al., Nucleoredoxin, glutaredoxin, and thioredoxin differentially regulate NF-κB, AP-1, and CREB activation in HEK293 cells, Biochem. Biophys. Res. Commun. 274 (2000) 177–182.
[59] D.Y. Jin, H.Z. Chae, S.G. Rhee, K.T. Jeang, Regulatory role for a novel human thioredoxin peroxidase in NF-κB activation, J. Biol. Chem. 272 (1997) 30952–30961.
[60] L. Zhang, Study on the Mechanism through Which HPD Regulate NF-κB Pathway and NLK Regulate TGFβ Pathway [D], PLA Academy of Military Medical Sciences, 2012.
[61] G.R. Moran, 4-Hydroxyphenylpyruvate dioxygenase, Arch. Biochem. Biophys. 433 (2005) 117–128.